Supporting Information

One-pot Cascade Conversion of Fructose to 2,5-Diformylfuran Enabled by a Polyionic Liquids based Porous Catalyst

Gang Liu[1,‡], Jun Zheng[1,‡], Xianqiang Huang[1]*, Shiqi Fu[1], Shiqi Xi[1], Yalin Zhang[1], Zhen Li[1], Fei Yu[3]* and Yifa Chen[2]*

[1] Shandong Provincial Key Laboratory of Chemical Energy Storage and Novel Cell Technology, School of Chemistry & Chemical Engineering, Liaocheng University, Liaocheng, Shandong, 252059, P. R. China.

[2] Guangdong Provincial Key Laboratory of Carbon Dioxide Resource Utilization, School of Chemistry, South China Normal University, Guangzhou 510006, P. R. China.

[3] Jiangsu Collaborative Innovation Centre of Biomedical Functional Materials, Jiangsu Key Laboratory of New Power Batteries, School of Chemistry and Materials Science, Nanjing Normal University, Nanjing, 210023, P. R. China.

‡ These authors contributed equally to this work.

Correspondence and requests for materials should be addressed to X. H. (email: hxq@lcu.edu.cn), F. Y. (email: feiyu@njnu.edu.cn), and Y. C. (email: chyf927821@163.com).

Materials and Methods

All the starting materials and organic solvents were purchased from commercial suppliers and used without further purification unless otherwise noted. The reagents and chemicals including 4-bromostyrene (98%), Mg (99.5%), fructose (98%), phosphorus tribromide (99%), dibromomethane (98%), HMF (96%), 1-vinylimidazole (98%), azobisisobutyronitrile (98%), imidazole (99.5%), sodium p-styrene sulfonate (95%), vanadium pentoxide (99.7%) etc. were all purchased from Energy Chemical and can be used directly without further purification.

Characterizations and instruments

The morphology and microstructure of the samples were observed by scanning electron microscopy (SEM, Thermo Fisher Scientific FIB-SEM GX4). Transmission electron microscopy (TEM) tests were conducted on a JEOL JEM-2100 electronmicroscope. The X-ray diffraction (PXRD) patterns were recorded on a Rigaku Smartlab3 X-ray Powder Diffractometer equipped with a Cu sealed tube (λ = 1.54178 Å) in the range of 5° to 50° at room temperature. The Fourier transform infrared spectrometry (FT-IR) analyses were measured on a Nicolet 5700 spectrophotometer in the range 400-4000 cm^{-1}. The X-ray photoelectron spectroscopy (XPS) C 1s and W 4f spectra of the samples were performed on Thermo Escalab Xi^{+}. The Raman spectra were obtained on a SNFT-SRLab1000. The UV-Vis spectroscopy was measured on UV-2600. ^{1}H NMR, ^{13}C NMR, distortionless enhancement by polarization transfer (DEPT) and attached proton test (APT) spectra were recorded on 500 MHz (Bruker) instrument, $CDCl_3$ (7.26 ppm for ^{1}H NMR, 77.16 ppm for ^{13}C NMR, 77.16 ppm for DEPT and 77.16 ppm for APT) was used as a reference. Data for ^{1}H were reported as follows: chemical shift (ppm), and multiplicity (s = singlet, d = doublet, t = triplet, q = quartet, dd = doublet of doublets, dt = doublet of triplets, m = multiplet and br = broad singlet). Column chromatography was hand packed with silica gel or aluminum oxide (200-300 mesh). The inductively coupled plasma-mass spectrometry (ICP-MS) analyses were performed on an Agilent 720. After the reaction was completed, the resulting mixture was finally analyzed by Waters E2695 HPLC (high performance liquid chromatography) with naphthalene as an internal standard. High-resolution mass spectra (HRMS) were recorded on a UPLC I-CLASS/XEVO G2-XS QTOF (ESI). TLC was carried out with 0.2 mm thick silica gel plates (GF254). Visualization was accomplished by UV light. The reactions were carried out in a high-pressure organic synthesis instrument (PPV-5460). The gram reaction is carried out in a high pressure reactor.

DFT calculations

DFT calculations were calculated using CP2K code (freely available at http://www.cp2k.org)[1], based on the mixed Gaussian and plane-wave scheme[2]and the Quickstep module.[3] The calculation used molecularly optimized Double-Zeta-Valence plus Polarization (DZVP) basis set,[4] Goedecker-Teter-Hutterpseudopotentials,[5] and the Perdew-Burke-Ernzerhof (PBE)[6] exchange correlation functional with the D3 dispersion corrections proposed by Grimme.[7] The plane-wave energy cutoff was 400 Ry. The calculation was performed on Gamma point only, with no symmetry constraint. Structural optimization was performed using the Broyden-Fletcher-Goldfarb-Shannon (BFGS) optimizer, until the maximum force is below 0.00045 Ry/Bohr (0.011 eV/Å). 30 Å of vacuum were included in the simulation cell to decouple the system from its periodic replicas in the direction perpendicular to the surface. To obtain the equilibrium geometries, we kept the atomic positions of the $PMo_{10}V_2$@2Br-PIL fixed base on the single crystal structures; all other atoms were relaxed until forces were lower than 0.005 eV $Å^{-1}$.

Synthesis of $PMo_{10}V_2$@2Br-PIL

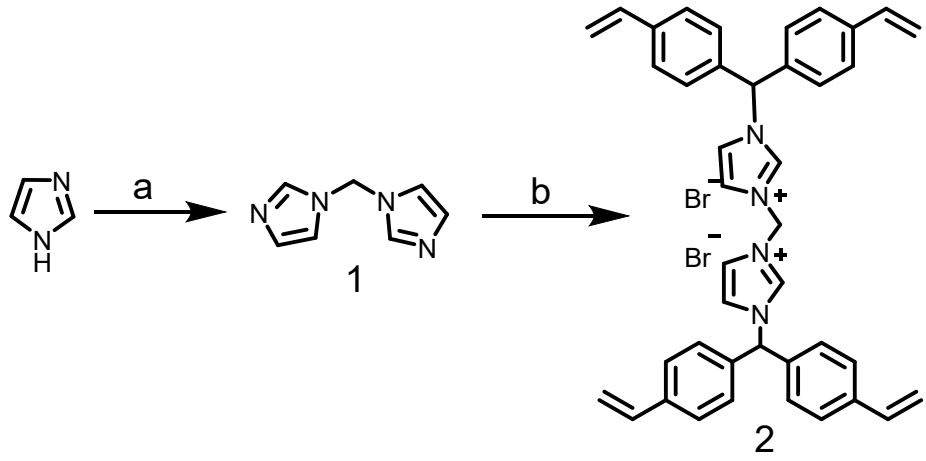

Di(1H-imidazol-1-yl)methane (1)

A mixture of imidazole (1.36 g) and tetrabuthylammoniumbromide (0.129 g, 0.400 mmol) in CH_2Cl_2 (30 mL) and 45% NaOH solution (11 mL) was stirred under reflux condition. After 16 h, the volatile was removed under reduced pressure. The residue was purified by flash column chromatography (CH_2Cl_2/MeOH = 10/1 to 4/1).[8] ^{1}H NMR (500 MHz, Chloroform-*d*) δ 7.66 (s, 2H), 7.12 (s, 2H), 6.99 (s, 2H), 6.01 (s, 2H).

3,3'-methylenebis(1-(bis(4-vinylphenyl)methyl)-1H-imidazol-3-ium) bromide salt (2)

4,4'-(Bromomethylene)bis(vinylbenzene) (**9**) (1 g) and di(1H-imidazol-1-yl)methane (0.4 g) was dissolved in acetone (20 mL), stirring at 60 °C under N_2 atmosphere for 12 h. After reaction, the mixture was cooled to room temperature and treared by filtration, washing with diethyl ether, and drying under vacuum at room temperature. The product was obtained as a white solid in quantitative yield. ^{1}H NMR (500 MHz, Chloroform-d) δ 10.94 (s, 2H), 9.21 (s, 2H), 7.59 (s, 2H), 7.45 (d, J = 7.8 Hz, 8H), 7.19 (d, J = 7.9 Hz, 8H), 7.04 (d, J = 21.5 Hz, 4H), 6.70 (d, J = 17.5 Hz, 4H), 5.80 (d, J = 17.6 Hz, 4H), 5.35 (d, J = 10.9 Hz, 4H). ^{13}C NMR (126 MHz, Chloroform-d) δ 138.97, 138.66, 135.71, 134.94, 128.70, 127.32, 124.09, 121.74, 115.99, 67.56.

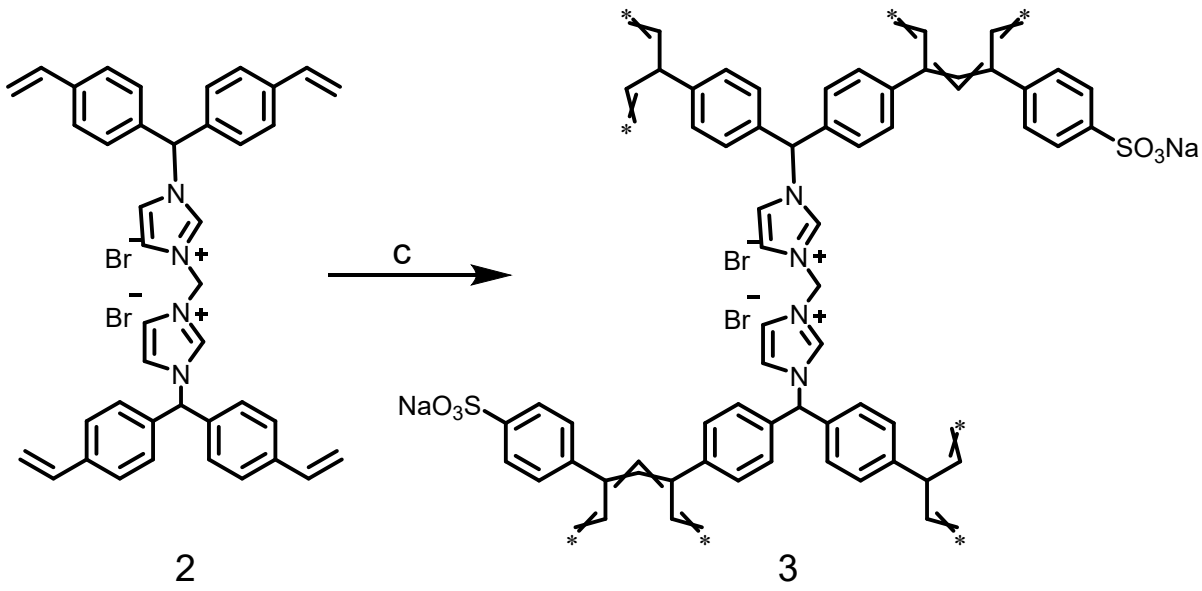

2 3

2Br-PIL (3)

As a typical run, **2** (300 mg) and 7 mg sodium p-styrene sulfonate were dissolved in 10 mL DMF, followed by the addition of 20 mg azobisisobutyronitrile (AIBN). The mixture was transferred into an autoclave at 100 °C for 24 h and washed with ethanol and dried under vacuum.

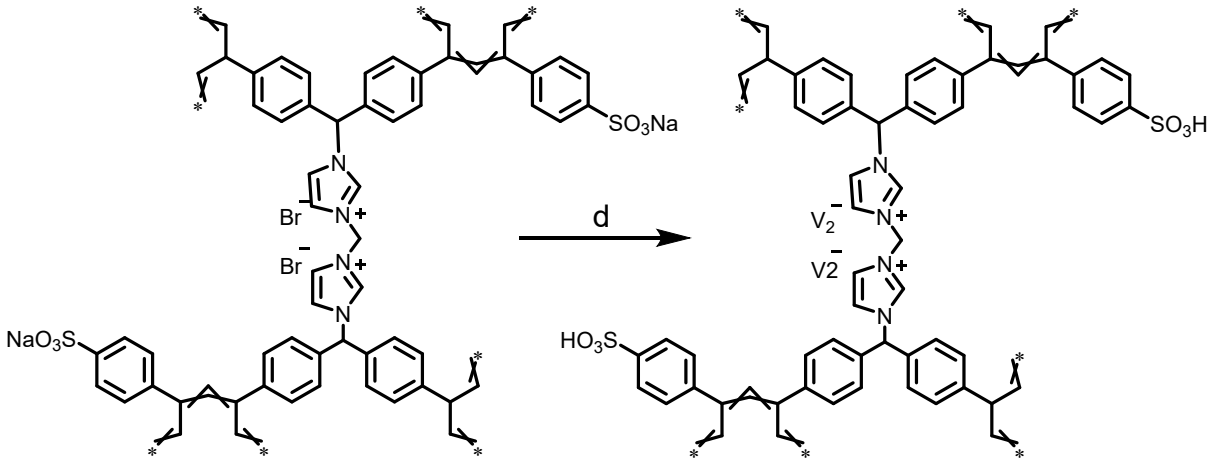

3 4

$PMo_{10}V_2$@2Br-PIL (4)

The yielded **3** was ion-exchanged using $H_5PMo_{10}V_2O_{40}$ (0.05, 0.1, 0.2, 0.3, 0.4 M) (30 mL) for 6 h and this procedure was repeated for three times. The resulting sample (denoted as $PMo_{10}V_2$@2Br-PIL) was washed with distilled water thoroughly until the pH of the filtrate was about 7 and then dried at 50 °C under vacuum for 12 h.

Synthesis of $PMo_{10}V_2$@Br-PIL

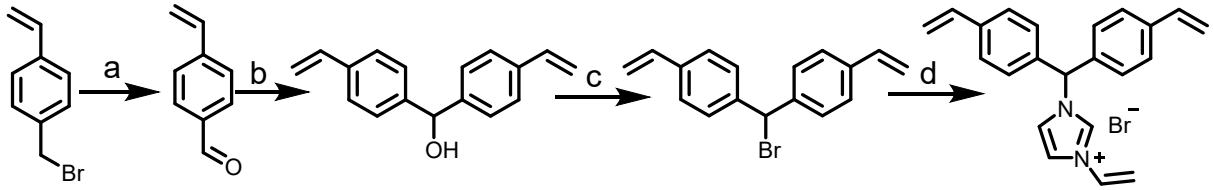

7 8 9 10

Vinylbenzaldehyde (7)

To a solution of (4-vinylphenyl)magnesium bromide, which was prepared by the reaction between 4-bromostyrene (100 mmol) and Mg powder (120 mmol) in 100 mL THF, DMF (150 mmol) was added dropwise at 0 °C under N_2 atmosphere. After stirring at room temperature overnight, the reaction was quenched by the addition of saturated NH_4Cl aqueous solution. The residue was extracted with ethyl acetate, washed with brine, dried over Na_2SO_4, and evaporated under reduced pressure. The crude compound was purified by flash chromatography on silica gel (hexane:EtOAc = 10:1) as eluent to afford the title compound as a kind of yellow oil. ^{1}H NMR (500 MHz, Chloroform-d) δ 9.96 (d, J = 2.3 Hz, 1H), 7.81 (d, J = 8.3 Hz, 2H), 7.66 – 7.47 (m, 2H), 6.74 (d, J = 17.6 Hz, 1H), 5.89 (d, J = 17.7 Hz, 1H), 5.41 (d, J = 11.0 Hz, 1H).

Bis(4-vinylphenyl)methanol (8)

To a solution of (4-vinylphenyl) magnesium bromide, which was prepared by the reaction of 4-bromostyrene (60 mmol) and Mg powder (72 mmol) in 100 mL THF, **7** (50 mmol) was added dropwise at 0 °C under N_2. After stirring at room temperature overnight, the reaction was

quenched by addition of saturated NH_4Cl aqueous solution. The residue was extracted with ethyl acetate, washed with brine, dried over Na_2SO_4, and evaporated underreduced pressure. The crude compound was purified by flash chromatography on silica gel (hexane:EtOAc = 10:1) as eluent to afford the title compound as a kind of white solid. ^{1}H NMR (500 MHz, Chloroform-*d*) δ 7.37 – 7.23 (m, 8H), 6.67 (d, *J* = 17.6 Hz, 2H), 5.76 – 5.66 (m, 3H), 5.21 (d, *J* = 10.9 Hz, 2H), 2.51 (s, 1H).

4,4'-(Bromomethylene)bis(vinylbenzene) (9)

PBr_3 (3.4 g) was added slowly to the solution of **8** (2.0 g) in 80 mL ether at 0 °C. The suspension was stirred at room temperature for 1 h, and then another portion of PBr_3 (3.4 g) was added. After stirring for another 1 h, the reaction was quenched by the addition of H_2O (100 mL). The residue was extracted with ether, washed with saturated $NaHCO_3$, and dried over Na_2SO_4. After the evaporation of the solvents, **9** as a kind of white solid was obtained. ^{1}H NMR (500 MHz, Chloroform-d) δ 7.47 – 7.32 (m, 8H), 6.70 (d, J = 17.6 Hz, 2H), 6.28 (s, 1H), 5.76 (d, J = 17.6 Hz, 2H), 5.27 (d, J = 10.9 Hz, 2H)[9].

1-(Bis(4-vinylphenyl)methyl)-3-vinylimidazolidine, bromide salt (10)

9 (2.0 g) and 1-vinylimidazole (0.7 g) were dissolved in acetone (20 mL) and stirred at 60 °C under N_2 atmosphere for 12 h. After reaction, the mixture was cooled to room temperature and treated by filtration, washing with diethyl ether, and drying under vacuum at room temperature. The product was obtained as a kind of white solid in quantitative yield. ^{1}H NMR (500 MHz, Chloroform-d) δ 11.00 (s, 1H), 7.64 (d, J = 6.2 Hz, 2H), 7.46 – 7.40 (m, 5H), 7.27 (d, J = 5.0 Hz, 4H), 7.17 (t, J = 1.9 Hz, 1H), 6.70 (d, J = 17.6 Hz, 2H), 5.92 (d, J = 15.6 Hz, 1H), 5.78 (d, J = 17.6 Hz, 2H), 5.43 (d, J = 8.6 Hz, 1H), 5.33 (d, J = 10.9 Hz, 2H).

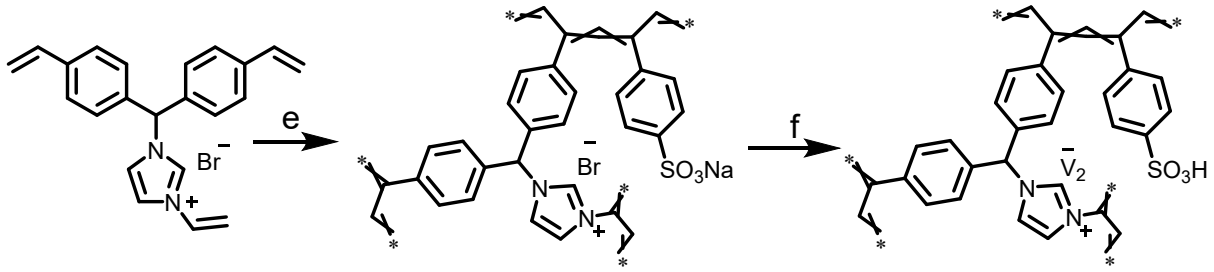

10 11 12

Br-PIL (11)

10 (1.0 g) and sodium p-styrene sulfonate (17 mg) were dissolved in 10 mL DMF, followed by the addition of 50 mg AIBN. The mixture was transferred into an autoclave at 100 °C for 24 h. The obtained product was washed with ethanol and dried under vacuum overnight.

$PMo_{10}V_2$@Br-PIL (12)

The yielded **11** was ion-exchanged using 0.2 M $PMo_{10}V_2$ (100 mL) for 6 h and this procedure was repeated for three times. The resulting sample was washed with distilled water thoroughly until the pH of the filtrate was about 7 and then dried at 50 °C under vacuum for 12 h to produce $PMo_{10}V_2$@Br-PIL.

One-pot transformation of fructose into DFF.

The 4 mmol fructose, 30 mg catalyst and 5 mL DMSO were added into the reactor. Then, the reactor was heated to 150 °C at 1.5 MPa O_2 under stirring for 10 h. Finally, the reactor was cooled down to RT. The catalyst was removed by filtration, and the solution of the reaction mixture was concentrated using rotary evaporation. The product was then purified by flash chromatography on neutral alumina using a mixture of petroleum ether/ethyl acetate (10:1 ~ 7:1) as the eluent, yielding the DFF and HMF products. ^{1}H NMR analysis of the DFF product revealed high purity, with only minor peaks corresponding to petroleum ether and ethyl acetate solvents, and no other byproducts were detected.

General procedure for the gram-scale experiment.

The 19.8 g fructose, 0.6 g catalyst and 150 mL DMSO were added into the reactor. Then, the reactor was heated to 150 °C at 1.5 MPa O_2 under stirring for 40 h. Finally, the reactor was cooled down to RT. The catalyst was removed by filtration, and the solution of the reaction mixture was concentrated using rotary evaporation. The product was then purified by flash chromatography on neutral alumina using a mixture of petroleum ether/ethyl acetate (10:1 ~ 7:1) as the eluent, yielding the DFF and HMF products. ^{1}H NMR analysis of the DFF product revealed high purity, with only minor peaks corresponding to petroleum ether and ethyl acetate solvents, and no other byproducts were detected.

Products Characterization.

The resulted solution after reaction was diluted with water, and filtered using PTFF filters, then the liquid sample was analyzed on a Waters 2998 PDA Delector HPLC with a Biorad aminex 87H column. The mobile phase was constituted of CH_3CN/H_2O solution at 1 mL/min. During the measurement, the temperature of the column was maintained at 35 ℃. The quantification of the reaction products was based on an external standard calibration curve method. The calibration curves were obtained by the measurement of pure compound.

The conversion of fructose (mol%), yields of the HMF and DFF were calculated as follows:

$$\text{Fructose conversion}=\left(1-\frac{Moles\ of\ fructose}{Moles\ of\ fructose\ loaded}\right)\times 100\%$$

$$\text{HMF yield}=\left(\frac{Moles\ of\ HMF}{Moles\ of\ fructose\ loaded}\right)\times 100\%$$

$$\text{DFF yield} = \left(\frac{Moles\ of\ DFF}{Moles\ of\ fructose\ loaded}\right) \times 100\%$$

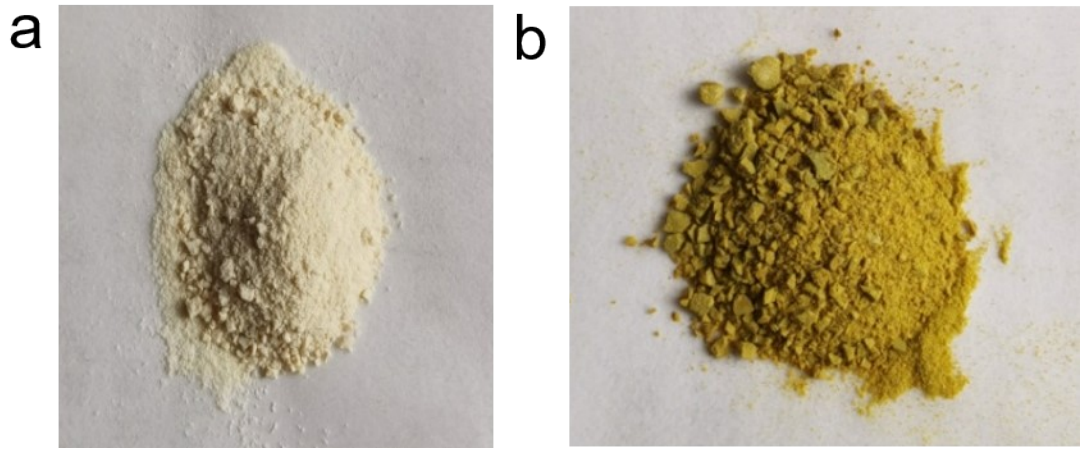

Figure S1. Images of catalysts. a) 2Br-PIL. b) $PMo_{10}V_2$@2Br-PIL.

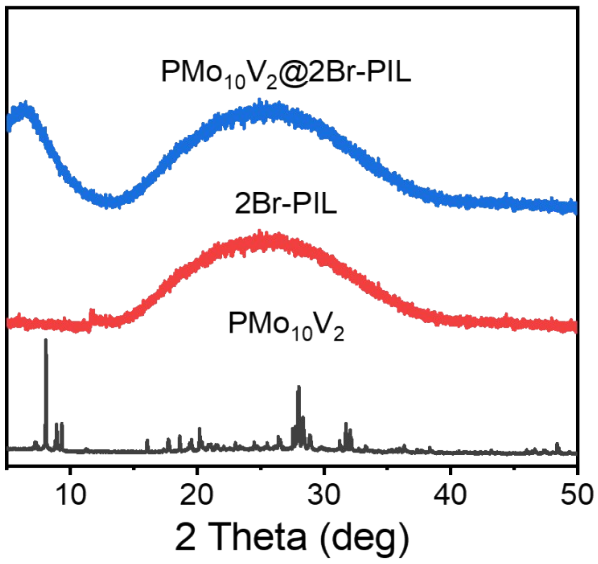

Figure S2. PXRD patterns of $PMo_{10}V_2$@2Br-PIL, 2Br-PIL and $PMo_{10}V_2$.

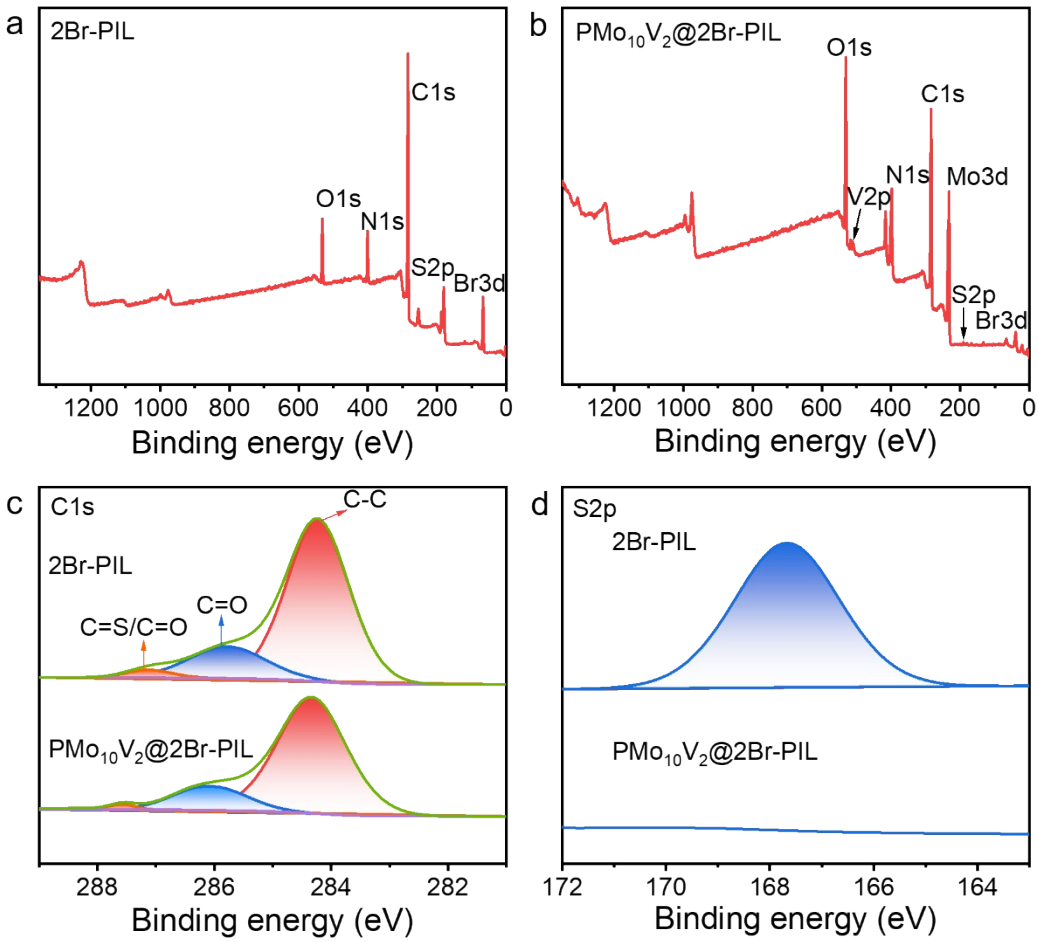

Figure S3. XPS spectra of $PMo_{10}V_2$@2Br-PIL and 2Br-PIL. a) Total XPS spectrum of 2Br-PIL; b) Total XPS spectrum of $PMo_{10}V_2$@2Br-PIL. c) XPS spectra of C1s for $PMo_{10}V_2$@2Br-PIL and 2Br-PIL. d) XPS spectra of S2p for $PMo_{10}V_2$@2Br-PIL and 2Br-PIL.

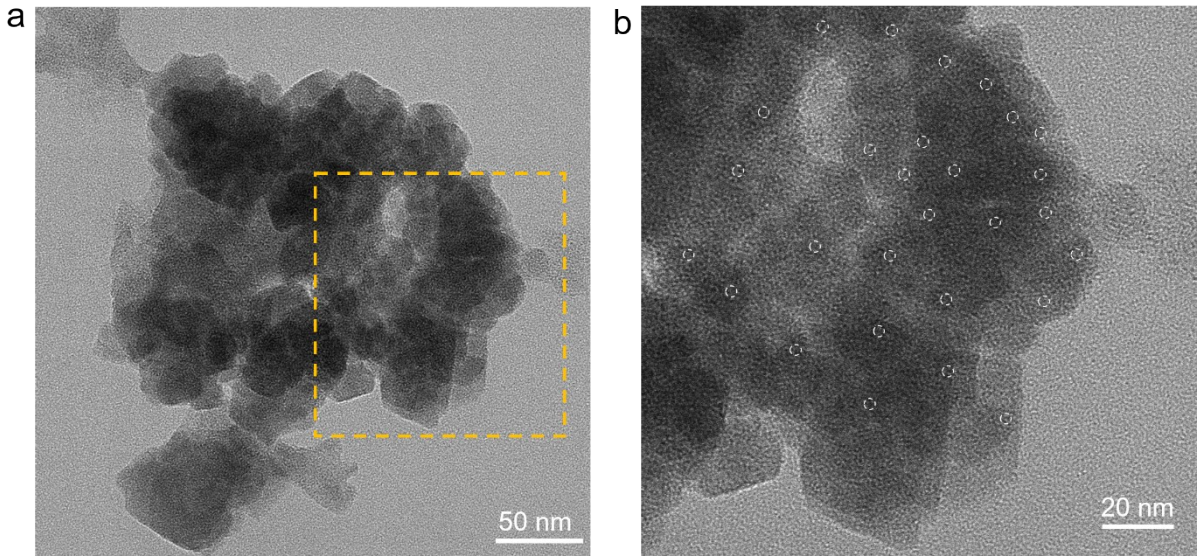

Figure S4. TEM images of $PMo_{10}V_2$@2Br-PIL. a) 50 nm. b) 20 nm.

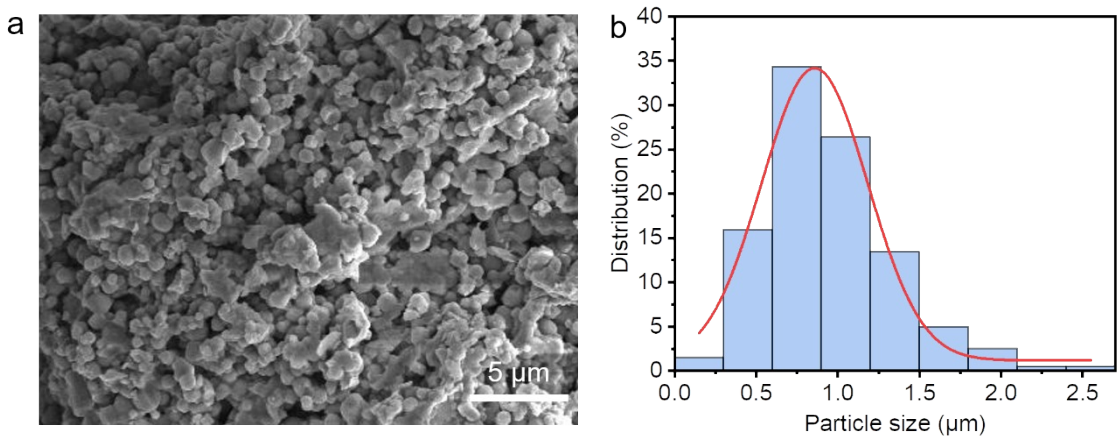

Figure S5. SEM and size-distribution histogram images of $PMo_{10}V_2$@2Br-PIL. a) SEM image. b) Size-distribution histogram.

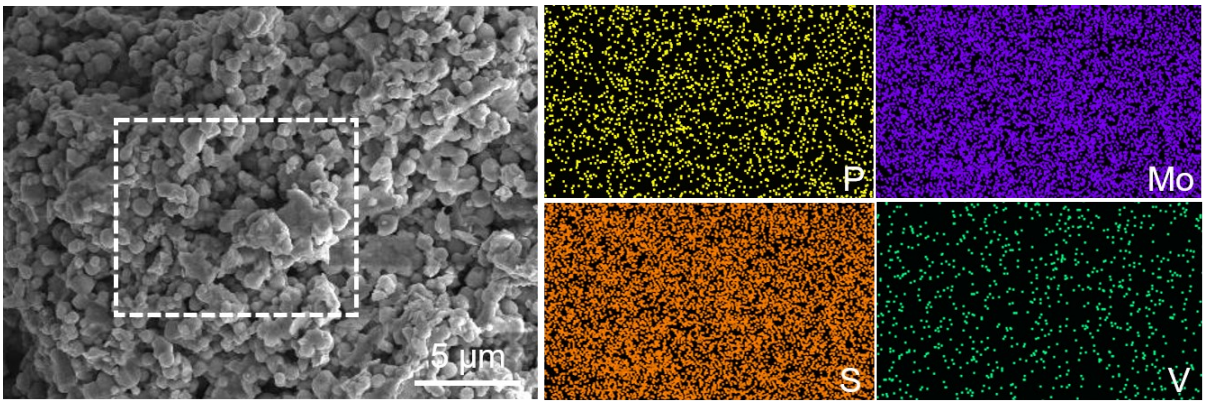

Figure S6. Elemental mapping image of $PMo_{10}V_2$@2Br-PIL.

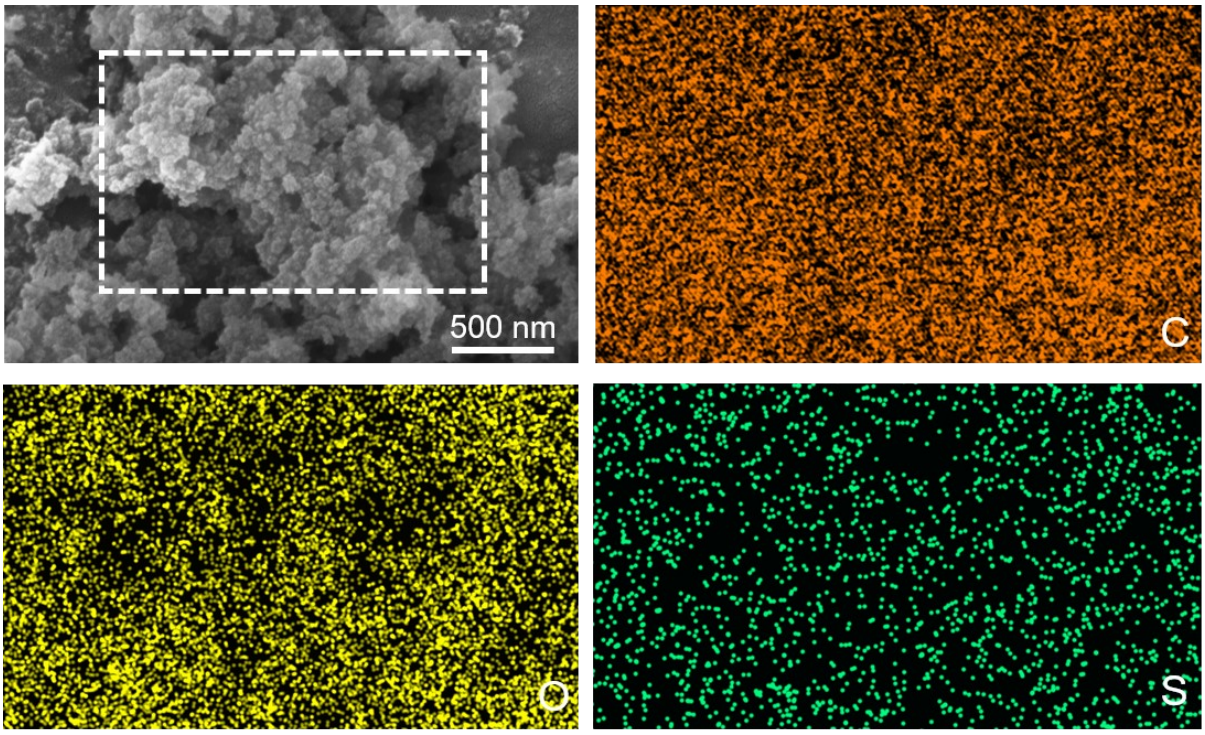

Figure S7. Elemental mapping image of 2Br-PIL.

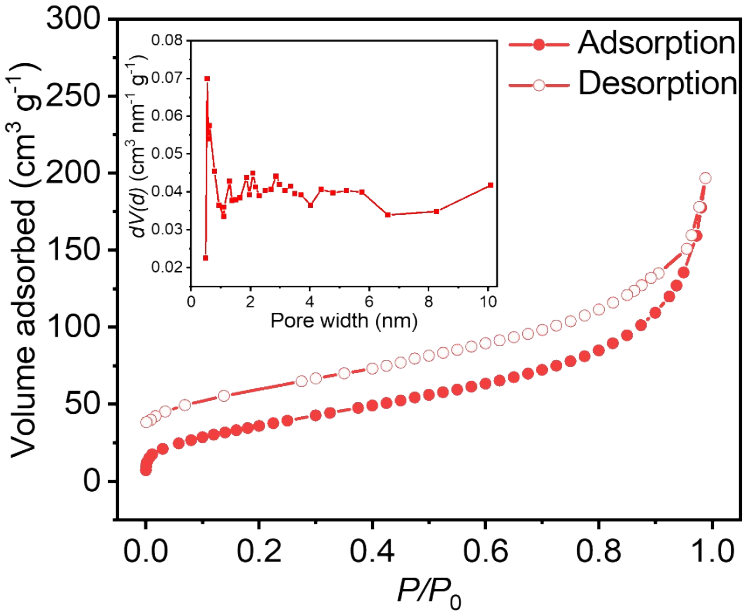

Figure S8. N_2 sorption isotherm of $PMo_{10}V_2$@2Br-PIL at 77 K (inset is the pore-size distribution profile).

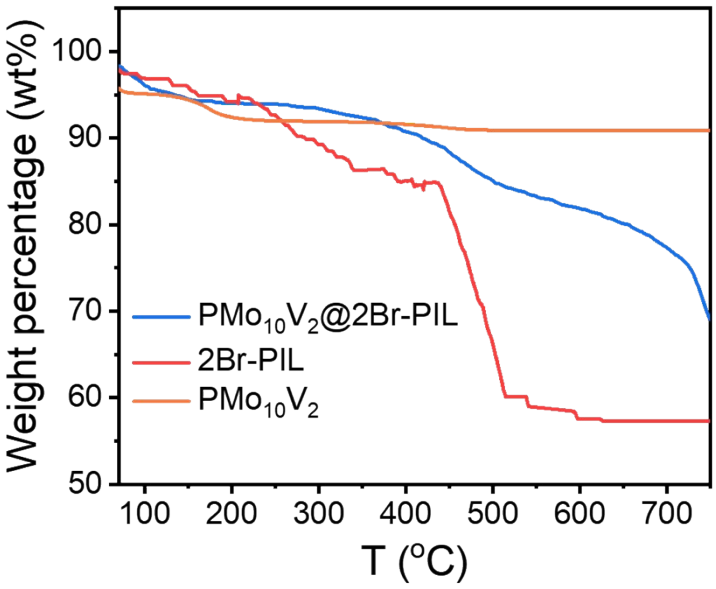

Figure S9. TGA of $PMo_{10}V_2$, 2Br-PIL and $PMo_{10}V_2$@2Br-PIL.

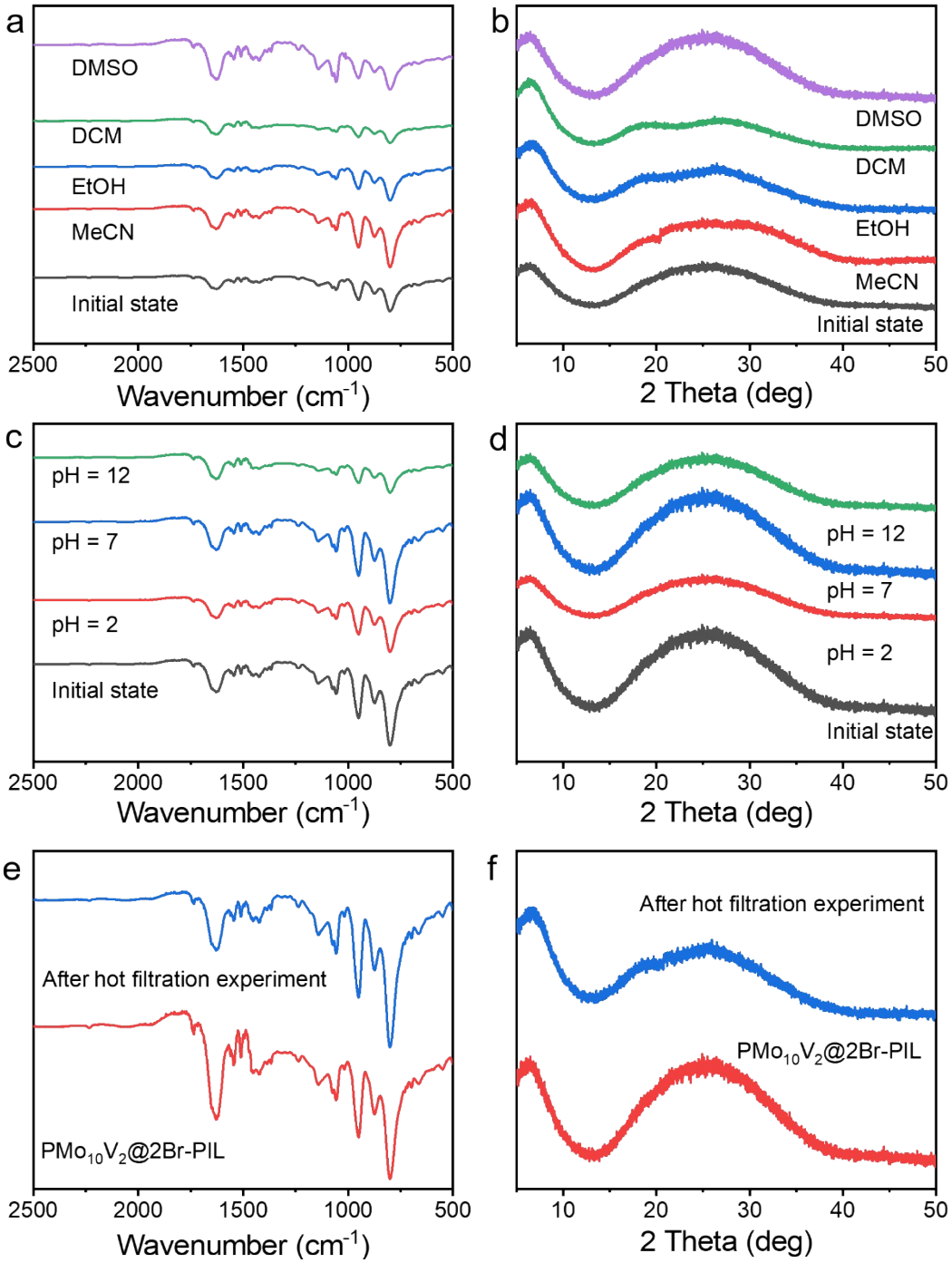

Figure S10. Stability tests of $PMo_{10}V_2$@2Br-PIL. a) FT-IR spectra and b) PXRD patterns of from leaching tests of $PMo_{10}V_2$@2Br-PIL after immersing in various solvents. c) FT-IR spectra and d) PXRD patterns of $PMo_{10}V_2$@2Br-PIL after immersing in the H_2O solutions with various pH values. e) FT-IR spectra and f) PXRD of $PMo_{10}V_2$@2Br-PIL hot filtration experiments.

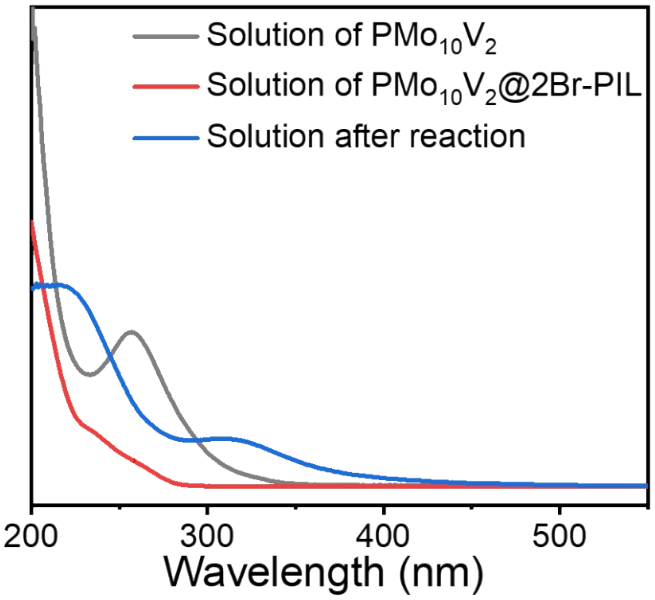

Figure S11. UV-vis spectra of solutions after immersing $PMo_{10}V_2$@2Br-PIL in it for 7 days (red) and after reaction (blue).

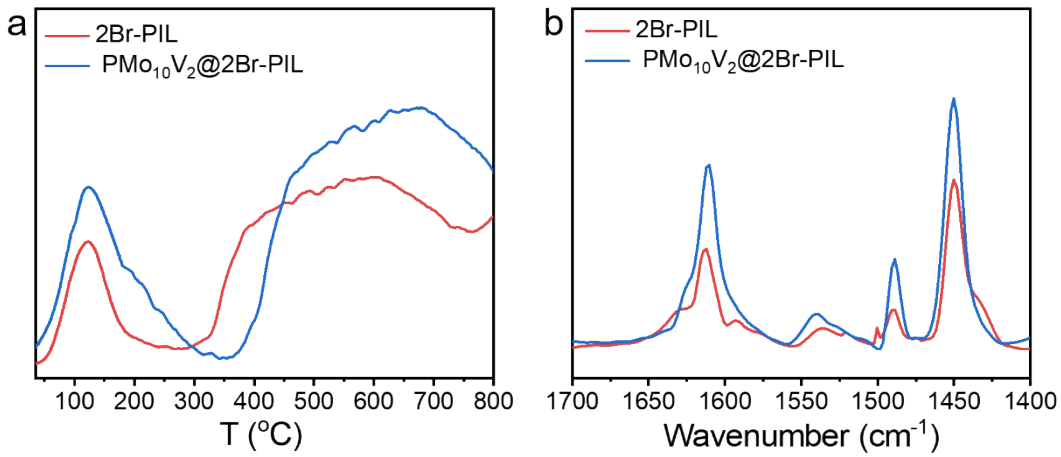

Figure S12. NH_3-TPD and pyridine-FTIR tests of $PMo_{10}V_2$@2Br-PIL with 2Br-PIL. a) NH_3-TPD. b) Pyridine-FTIR (150 °C).

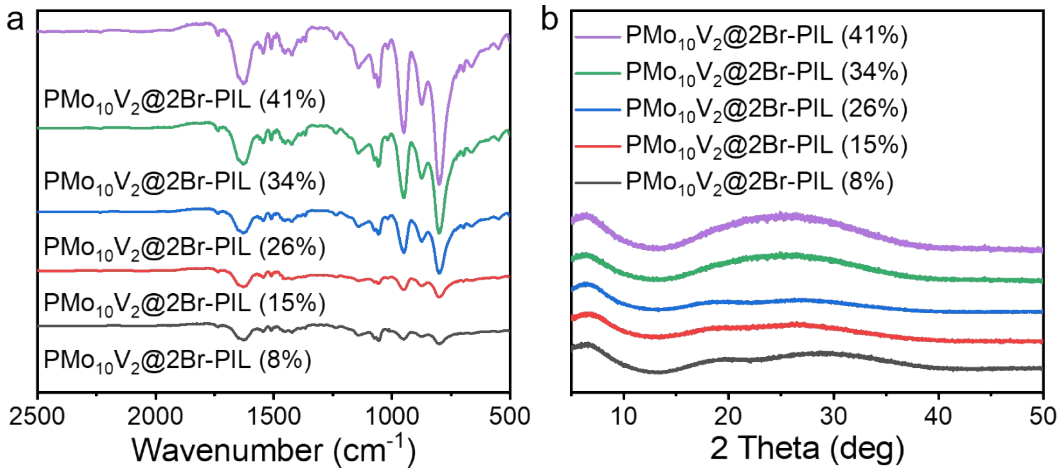

Figure S13. FT-IR spectra and PXRD patterns of $PMo_{10}V_2$@2Br-PIL with various $PMo_{10}V_2$ loadings. a) FT-IR spectra. b) PXRD patterns.

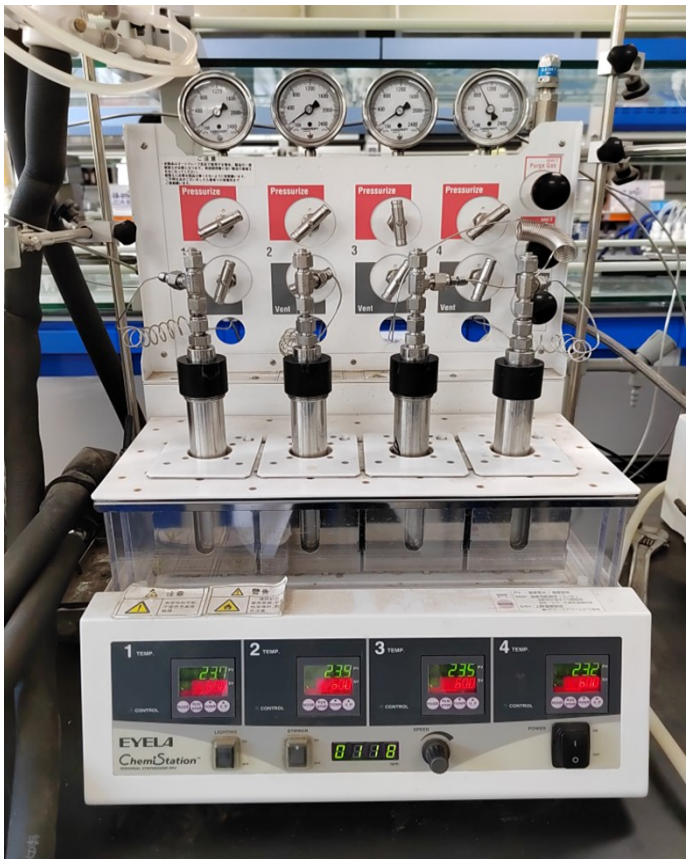

Figure S14. The device for the fructose into DFF by $PMo_{10}V_2$@2Br-PIL.

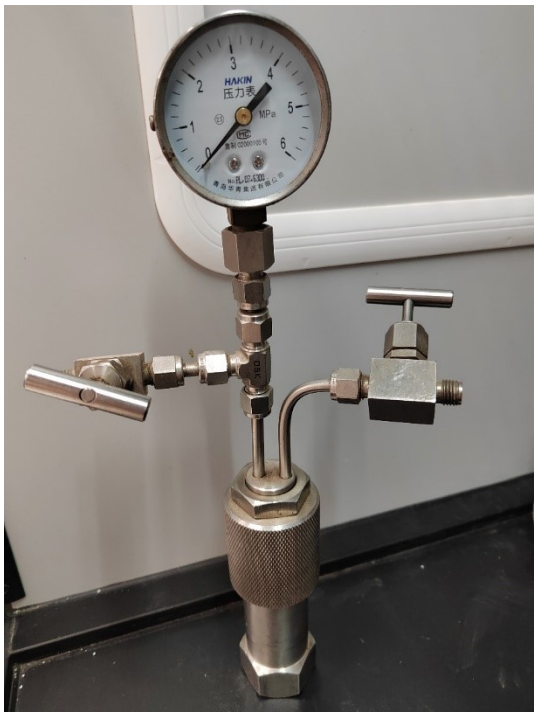

Figure S15. The device for the large scale experiment of DFF by $PMo_{10}V_2$@2Br-PIL (110 mmol, 27.5 equivalent).

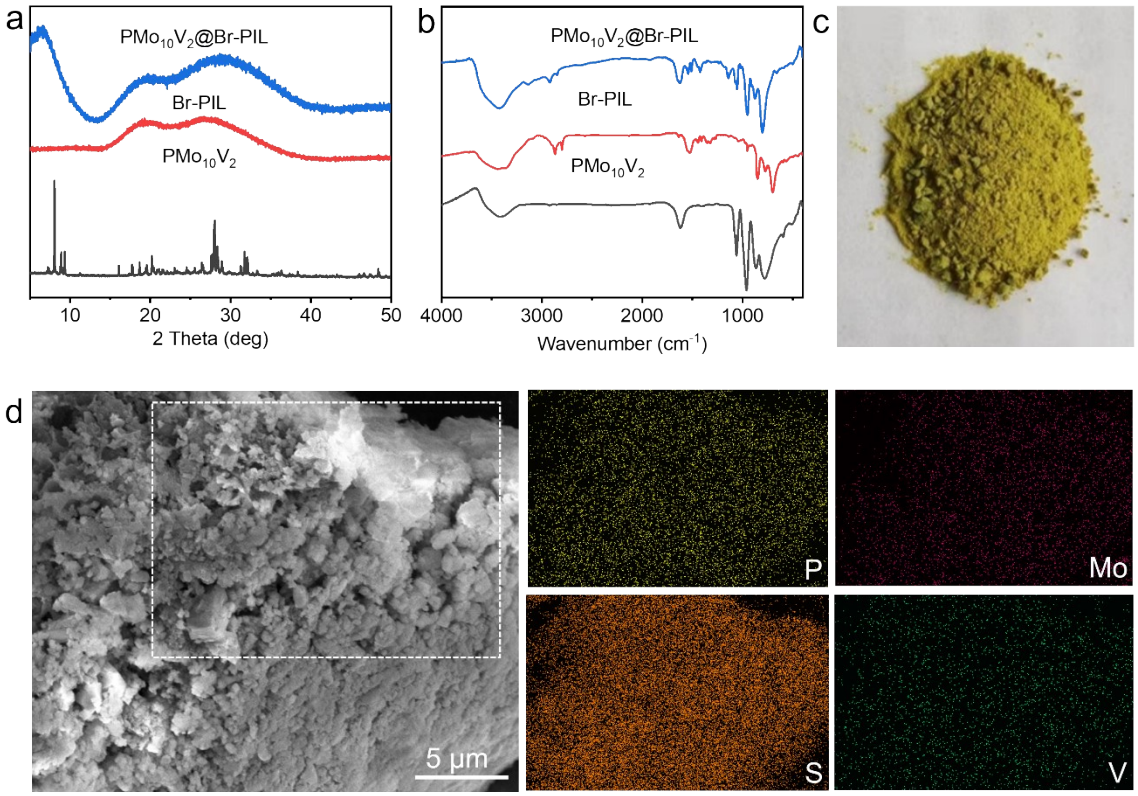

Figure S16. The characterization of $PMo_{10}V_2$@Br-PIL. a) FT-IR spectra of $PMo_{10}V_2$@Br-PIL, Br-PIL and $PMo_{10}V_2$. b) PXRD patterns of $PMo_{10}V_2$@Br-PIL, Br-PIL and $PMo_{10}V_2$. c) Picture of $PMo_{10}V_2$@Br-PIL. d) Elemental mapping image of $PMo_{10}V_2$@Br-PIL.

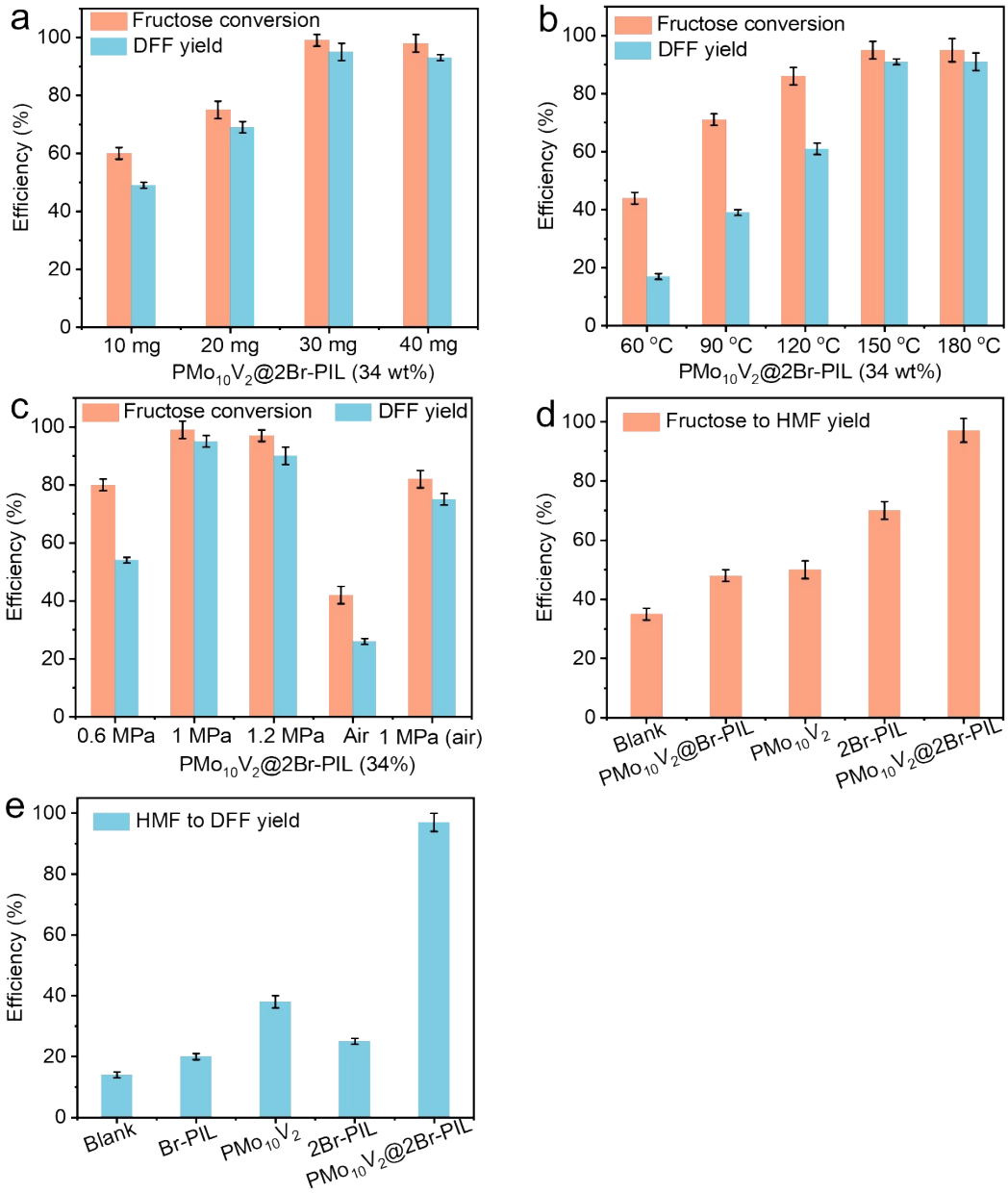

Figure S17. Optimization of reaction conditions on the model reaction. a) The efficiency of $PMo_{10}V_2$@2Br-PIL (34 wt%) with different amounts. b) The efficiency of $PMo_{10}V_2$@2Br-PIL (34 wt%) at different temperatures. c) The efficiency of $PMo_{10}V_2$@2Br-PIL (34 wt%) under different pressures. d) The efficiency of various catalysts on the fructose into HMF reaction (120 °C, N_2, 2 h). e) The efficiency of various catalysts on the HMF into DFF reaction (1 MPa O_2, 7 h). Reaction conditions: 4 mmol fructose, 30 mg catalyst, 5 mL DMSO, 150 °C, 1.5 MPa O_2, 10 h.

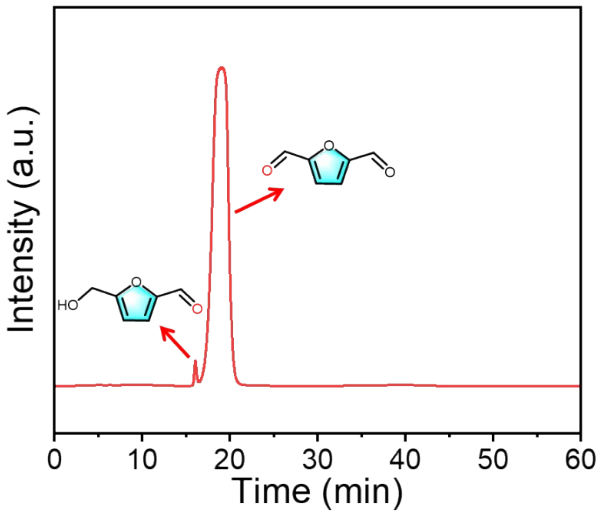

Figure S18. HPLC spectrum of the fructose oxidation catalyzed by $PMo_{10}V_2$@2Br-PIL.

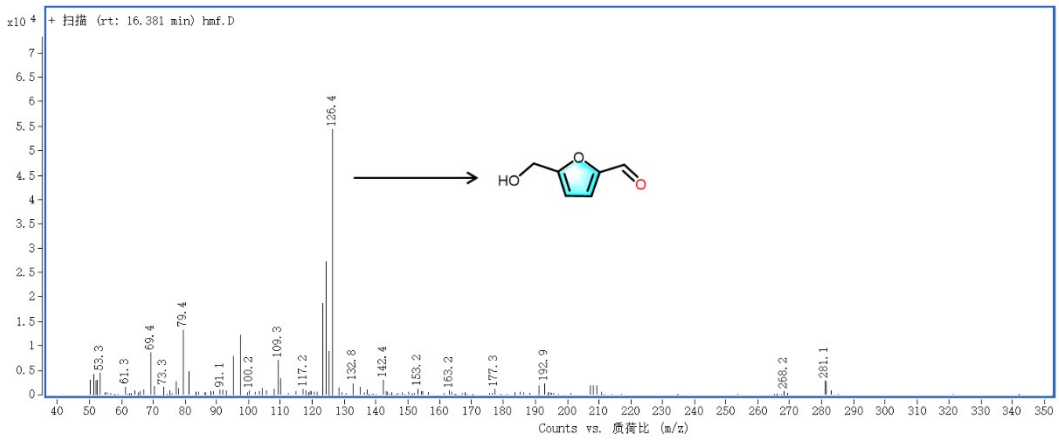

Figure S19. MS spectrum of DFF.

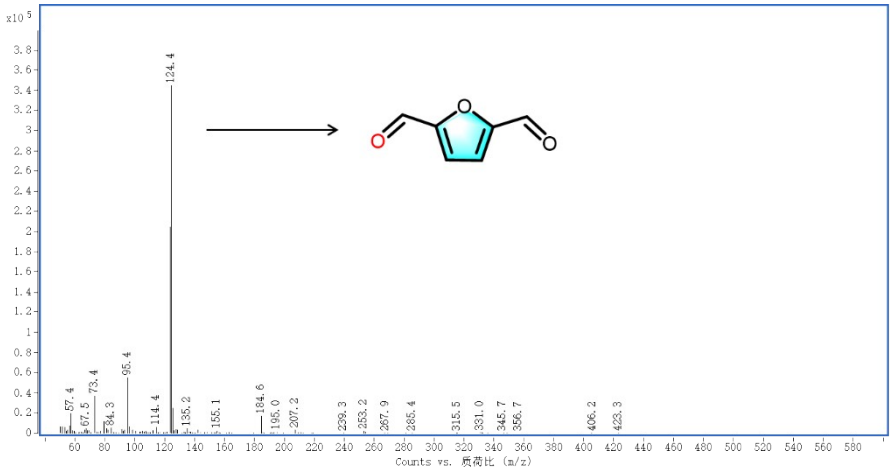

Figure S20. MS spectrum of DFF.

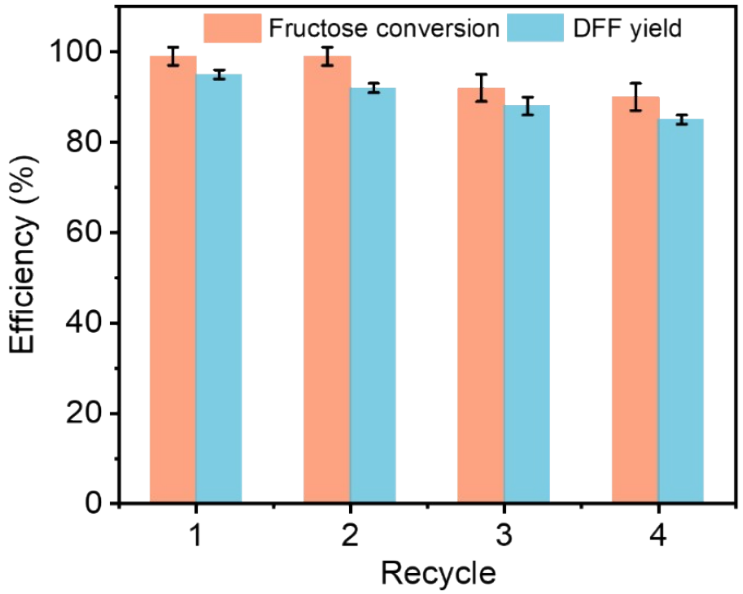

Figure S21. Reusability of $PMo_{10}V_2$@2Br-PIL.

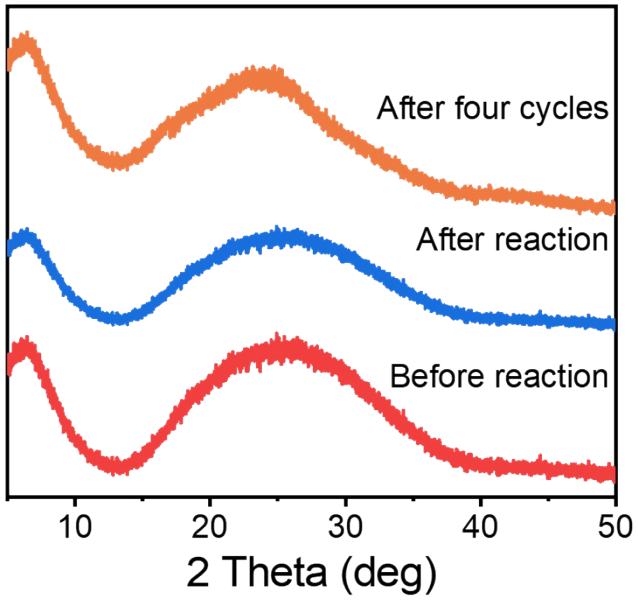

Figure S22. PXRD patterns of $PMo_{10}V_2$@2Br-PIL before and after reactions.

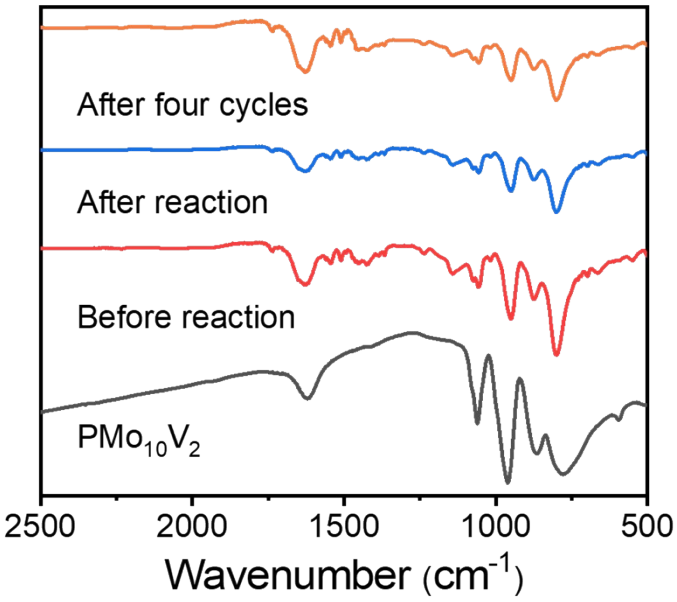

Figure S23. FT-IR spectra of $PMo_{10}V_2$@2Br-PIL before and after reactions.

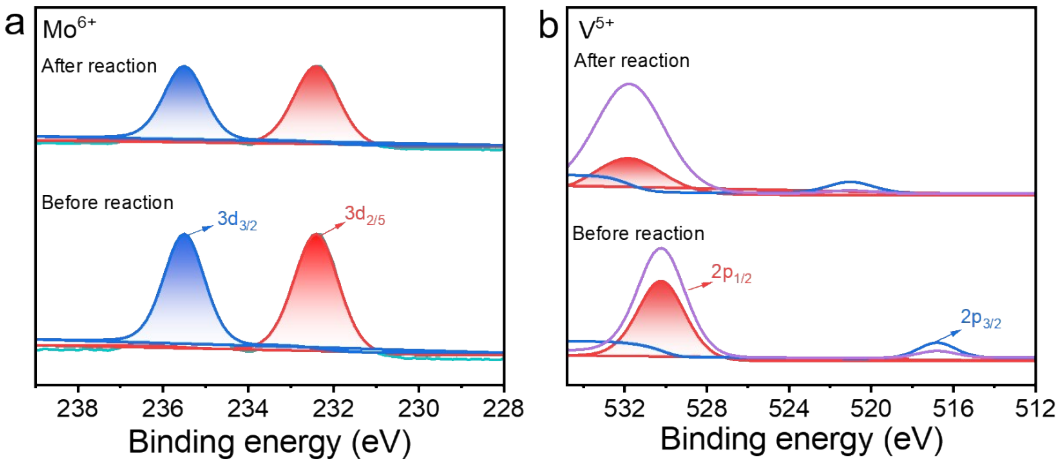

Figure S24. XPS spectra of $PMo_{10}V_2$@2Br-PIL before and after reactions. a) XPS spectra of Mo 3d for before and after reactions. b) XPS spectra of V 2p for before and after reactions.

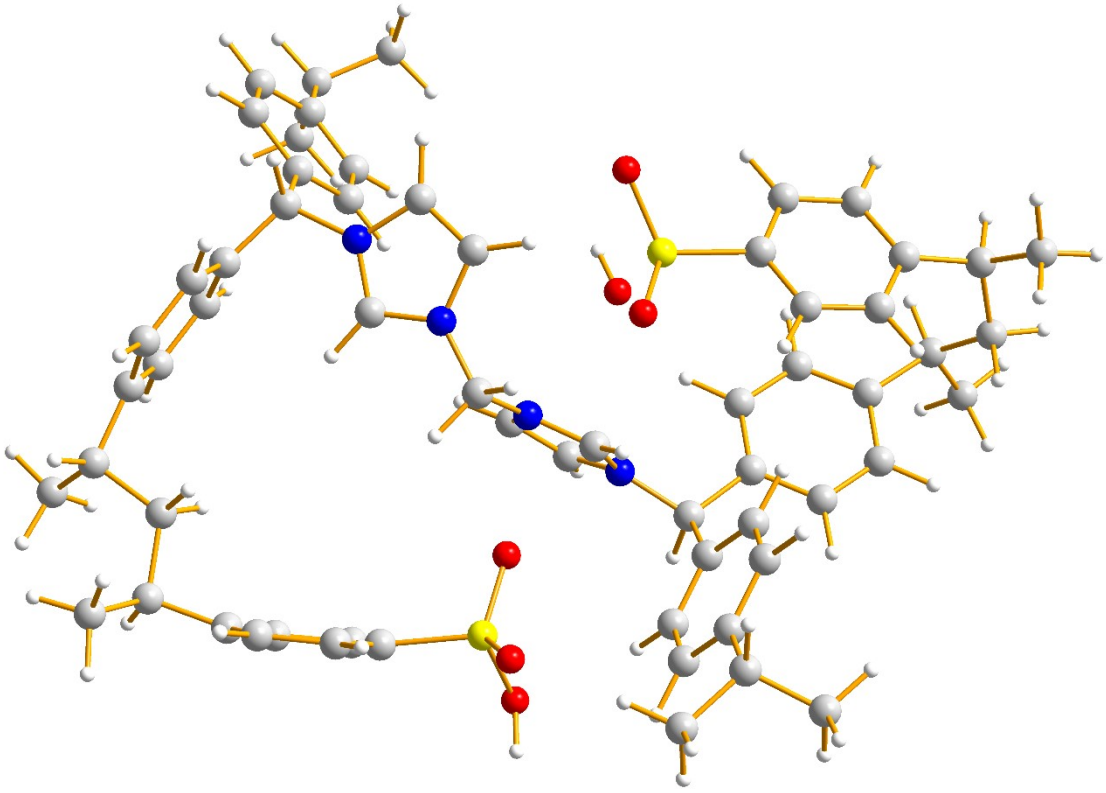

Figure S25. Schematic diagram of DFT calculation for 2Br-PIL unit.

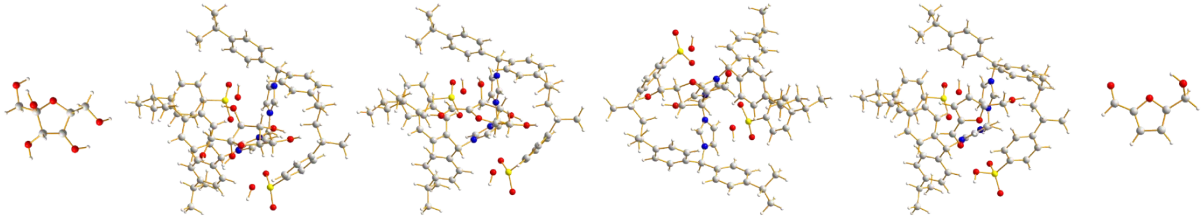

Figure S26. Schematic diagram of DFT calculations for substrate, intermediate and product on 2Br-PIL unit.

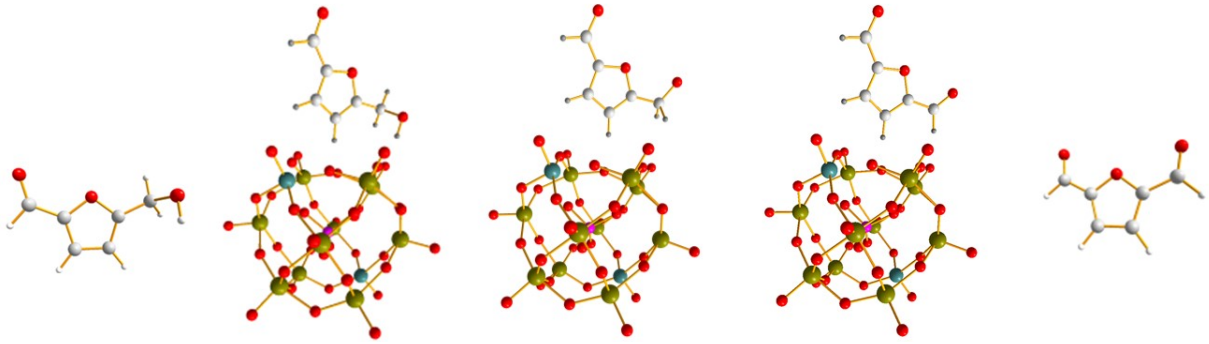

Figure S27. Schematic diagram of DFT calculations for HMF, intermediate and product on $PMo_{10}V_2$ unit.

Table S2. Performance of biomass-to-DFF by $PMo_{10}V_2$@2Br-PIL and reported catalysts.

Substrate	Reaction conditions	Catalysts	Yield (%)	TOF (μmol g^{-1} h^{-1})	Ref.
Fructose	DMSO, O_2, 150 °C.	$PMo_{10}V_2$@2Br-PIL	95	12668	This work
HMF	O_2, blue LED	Cu-SAs/p-CNS	66	2640	Adv. Mater., 2021, **33**, 2105904.
HMF	LED 450 nm, O_2, MeCN	$MAPbBr_3$	90	11250	ACS Catal., 2020, **10**, 14793-14800.
HMF	NIR light (850 nm), 50 °C, 1 M NaOH, HMF	MoS_2	10	980	Sci. Adv., 2024, **10**, 9441.
HMF	300 W Xe lamp with BUV bulb (380-800 nm), 0.2 MPa	CuCoAl-LDHs-E-60	87.32	10.40	Chem Catal., 2022, **2**, 531-549.
Fructose	Ethanol, 100 °C, N_2 for 2 h and then changed to O_2 for 3 h	Fe/C-S	54	9671.64	Green Chem., 2017, **19**, 647-655
Glucose	160 °C, H_2O/THF	[MimAM] $H_2PW_{12}O_{40}$	53.9	440	Green Chem., 2018, **20** 1551-1559.
Fructose	H_2O, 160 °C, 1 MPa air	Ru/S-rGO	47	11086.13	Chem. Eng. J., 2020, **379**, 122284.
Fructose	DMSO, O_2, 130 °C	MoO_x/CS-air	78	12580	ACS Sustainable Chem. Eng. 2019, **7**, 315-323.
Fructose	KBr, 120 °C	Amberlite IR 120 H	80	1480	Green Chem., 2022, **24**, 6125-6130.
Fructose	DMSO, O_2, 150 °C	MoO_3-ZrO_2	74	2529.41	ACS Sustainable Chem. Eng. 2018, **6**, 2976-2982.
Fructose	DMSO, O_2, 150 °C	Mo-HNC	77	2374.17	ACS Sustainable Chem. Eng. 2018, **6**, 284-291.
Fructose	DMSO, 140 °C, O_2 (0.8 MPa)	HPMoV/CS-f (25)	61.9	1352.78	ChemSusChem 2019, **12**, 3515-3523.

Table S2. ICP-MS and elemental analyses of V and S contents in $PMo_{10}V_2$@2Br-PIL

Substrate	ICP-MS (Mo)	ICP-MS (V)	Elemental analyses (S)
Before reaction	4.5431%	0.8908%	0.02083%
After reaction	4.4493%	0.8528%	0.0199%

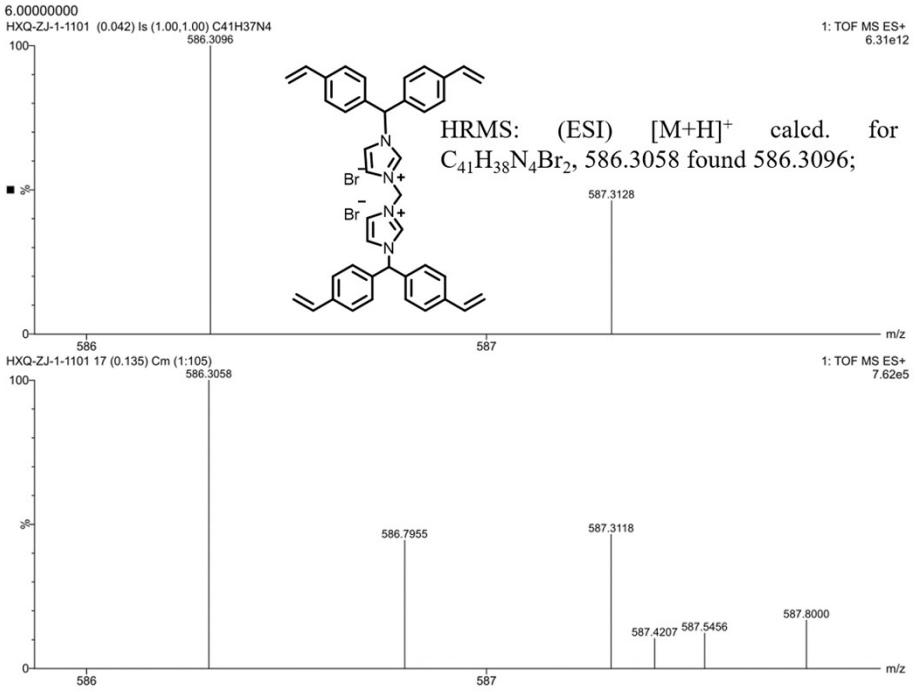

Figure S28. LC-MS experimental data of the intermediate **2**.

Characterization data of the products

4-vinylbenzaldehyde:

^{1}H NMR (500 MHz, Chloroform-*d*) δ 9.96 (d, *J* = 2.3 Hz, 1H), 7.81 (dd, *J* = 8.3, 2.2 Hz, 2H), 7.66 – 7.47 (m, 2H), 6.74 (ddd, *J* = 17.6, 10.9, 2.3 Hz, 1H), 5.89 (dd, *J* = 17.7, 2.3 Hz, 1H), 5.41 (dd, *J* = 11.0, 2.3 Hz, 1H).

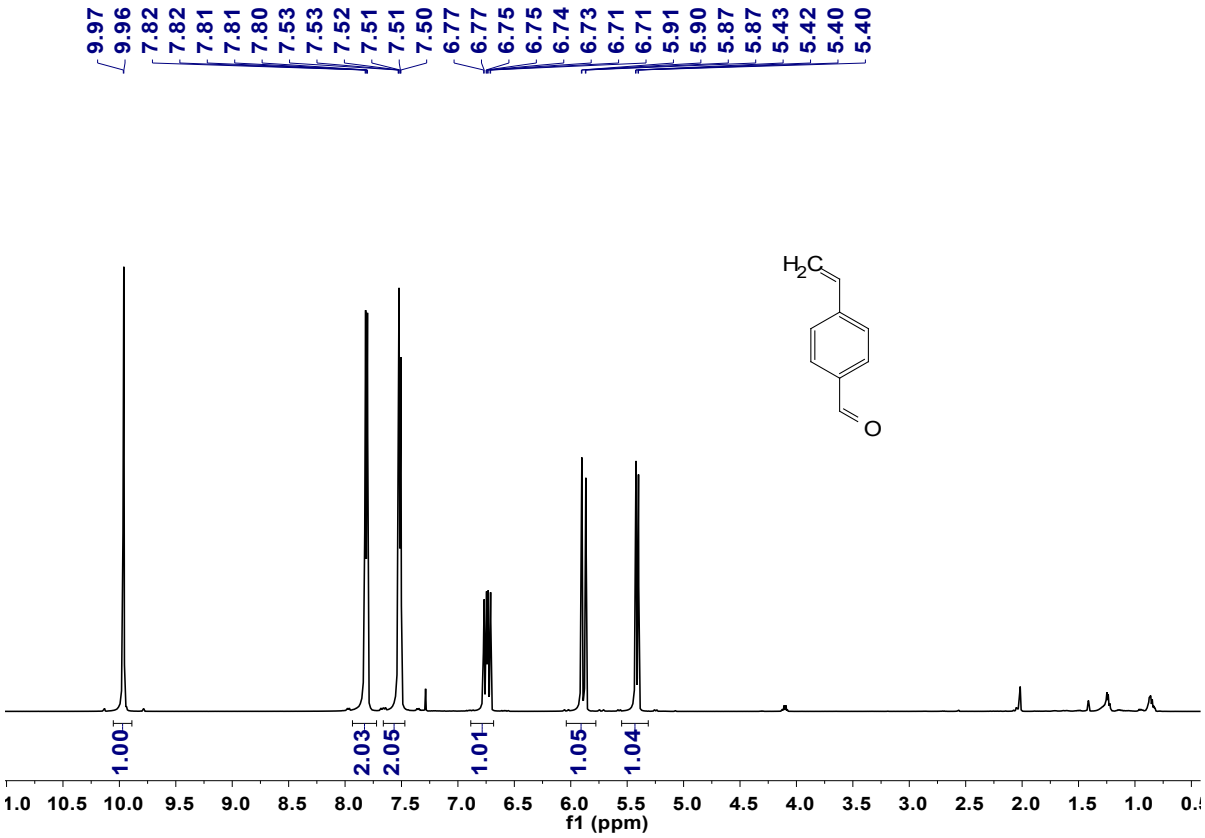

Figure S29. ^{1}H NMR spectra of compound **7**.

bis(4-vinylphenyl)methanol:

^{1}H NMR (500 MHz, Chloroform-*d*) δ 7.37 – 7.23 (m, 8H), 6.67 (dd, *J* = 17.6, 10.9 Hz, 2H), 5.76 – 5.66 (m, 3H), 5.21 (d, *J* = 10.9 Hz, 2H), 2.51 (s, 1H).

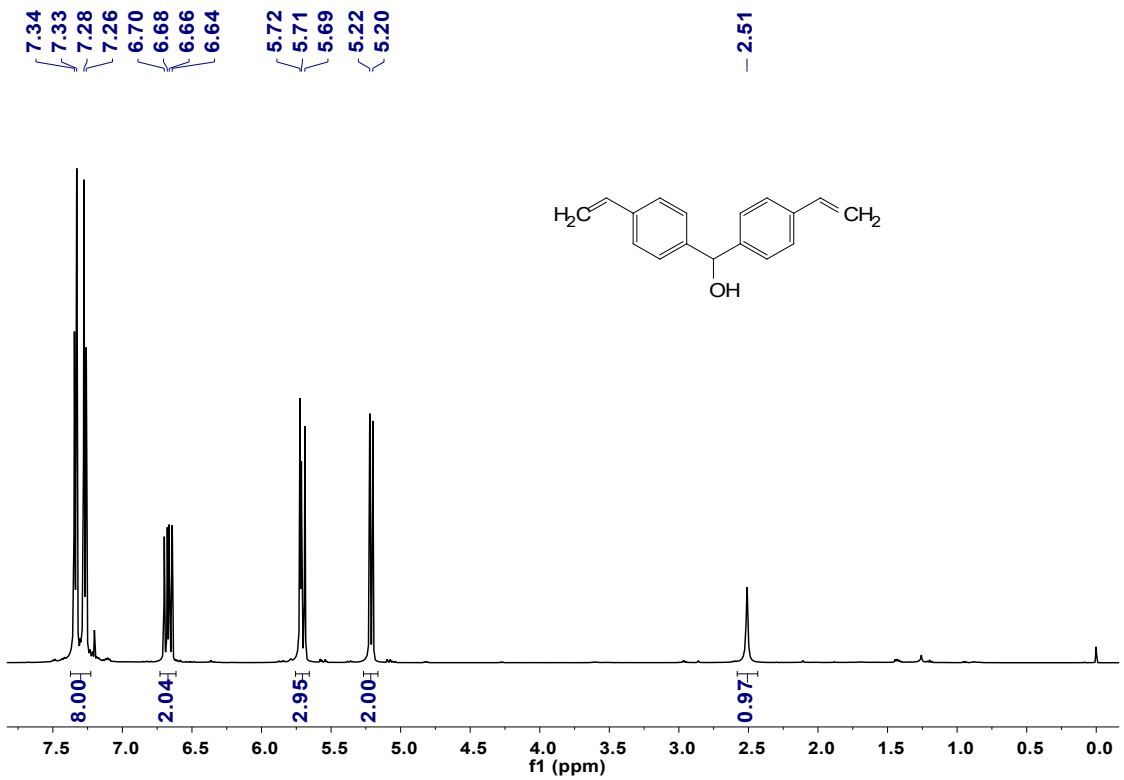

Figure S30. ^{1}H NMR spectra of compound **8**.

4,4'-(bromomethylene)bis(vinylbenzene):

^{1}H NMR (500 MHz, Chloroform-*d*) δ 7.47 – 7.32 (m, 8H), 6.70 (dd, *J* = 17.6, 10.9 Hz, 2H), 6.28 (s, 1H), 5.76 (d, *J* = 17.6 Hz, 2H), 5.27 (d, *J* = 10.9 Hz, 2H).

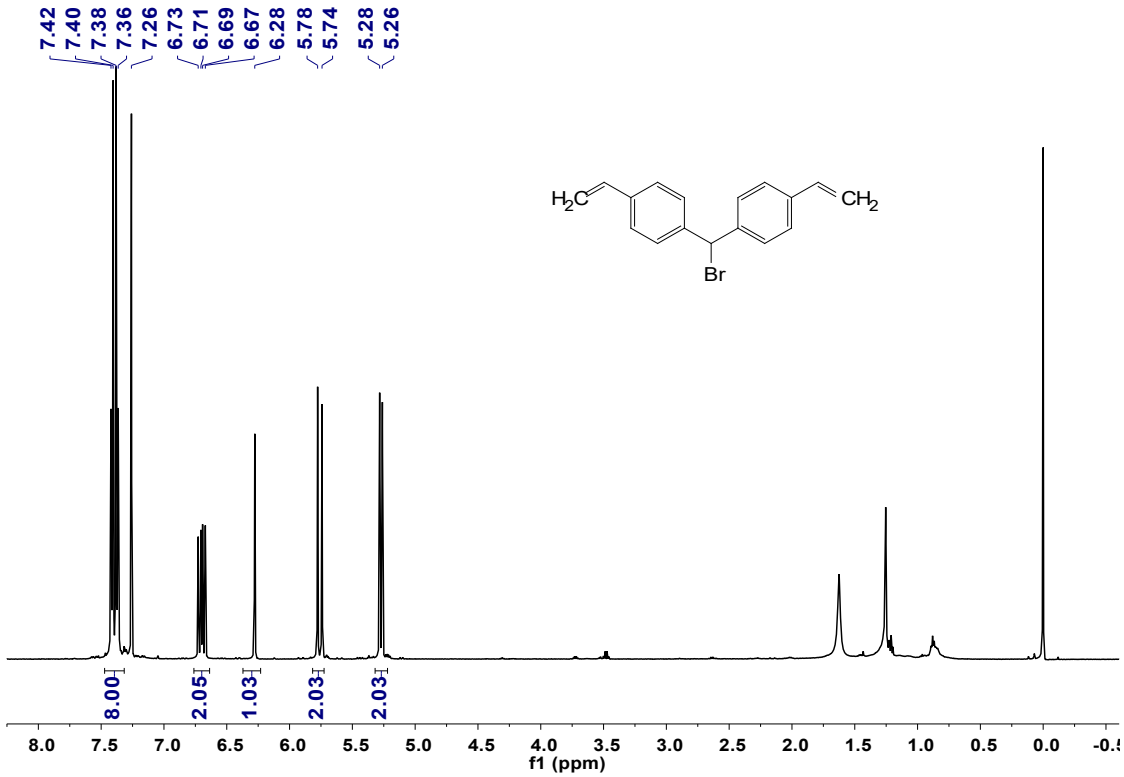

Figure S31. ^{1}H NMR spectra of compound **9**.

1-(bis(4-vinylphenyl)methyl)-3-vinyl-1H-imidazol-3-ium:

^{1}H NMR (500 MHz, Chloroform-*d*) δ 11.00 (s, 1H), 7.64 (d, *J* = 6.2 Hz, 2H), 7.46 – 7.40 (m, 5H), 7.27 (d, *J* = 5.0 Hz, 4H), 7.17 (t, *J* = 1.9 Hz, 1H), 6.70 (dd, *J* = 17.6, 10.9 Hz, 2H), 5.92 (dd, *J* = 15.6, 3.1 Hz, 1H), 5.78 (dd, *J* = 17.6, 0.8 Hz, 2H), 5.43 (dd, *J* = 8.6, 3.1 Hz, 1H), 5.33 (dd, *J* = 10.9, 0.7 Hz, 2H).

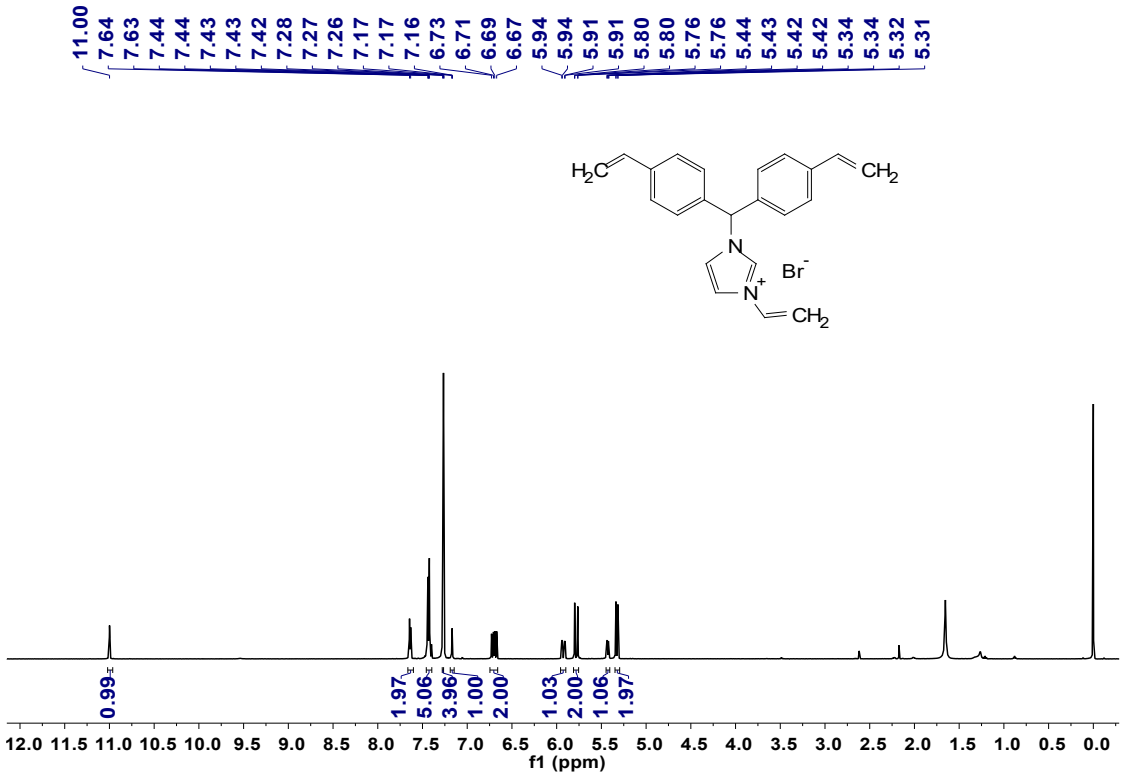

Figure S32. ^{1}H NMR spectra of compound **10**.

di(1H-imidazol-1-yl)methane:

^{1}H NMR (500 MHz, Chloroform-*d*) δ 7.66 (s, 2H), 7.12 (s, 2H), 6.99 (s, 2H), 6.01 (s, 2H).

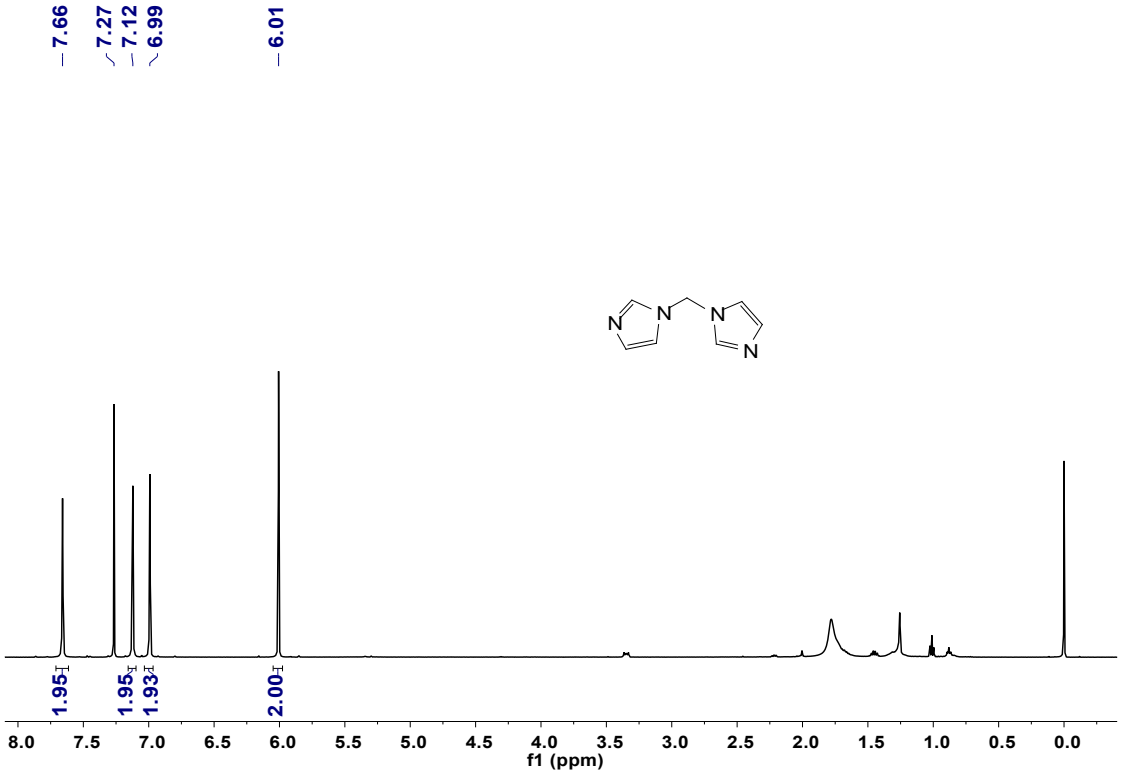

Figure S33. ^{1}H NMR spectra of compound **1**.

3,3'-methylenebis(1-(bis(4-vinylphenyl)methyl)-1H-imidazol-3-ium):

^{1}H NMR (500 MHz, Chloroform-*d*) δ 10.94 (s, 2H), 9.21 (s, 2H), 7.59 (s, 2H), 7.45 (d, *J* = 7.8 Hz, 8H), 7.19 (d, *J* = 7.9 Hz, 8H), 7.04 (d, *J* = 21.5 Hz, 4H), 6.70 (d, *J* = 17.5 Hz, 4H), 5.80 (d, *J* = 17.6 Hz, 4H), 5.35 (d, *J* = 10.9 Hz, 4H). ^{13}C NMR (126 MHz, Chloroform-*d*) δ 138.97, 138.66, 135.71, 134.94, 128.70, 127.32, 124.09, 121.74, 115.99, 67.56.

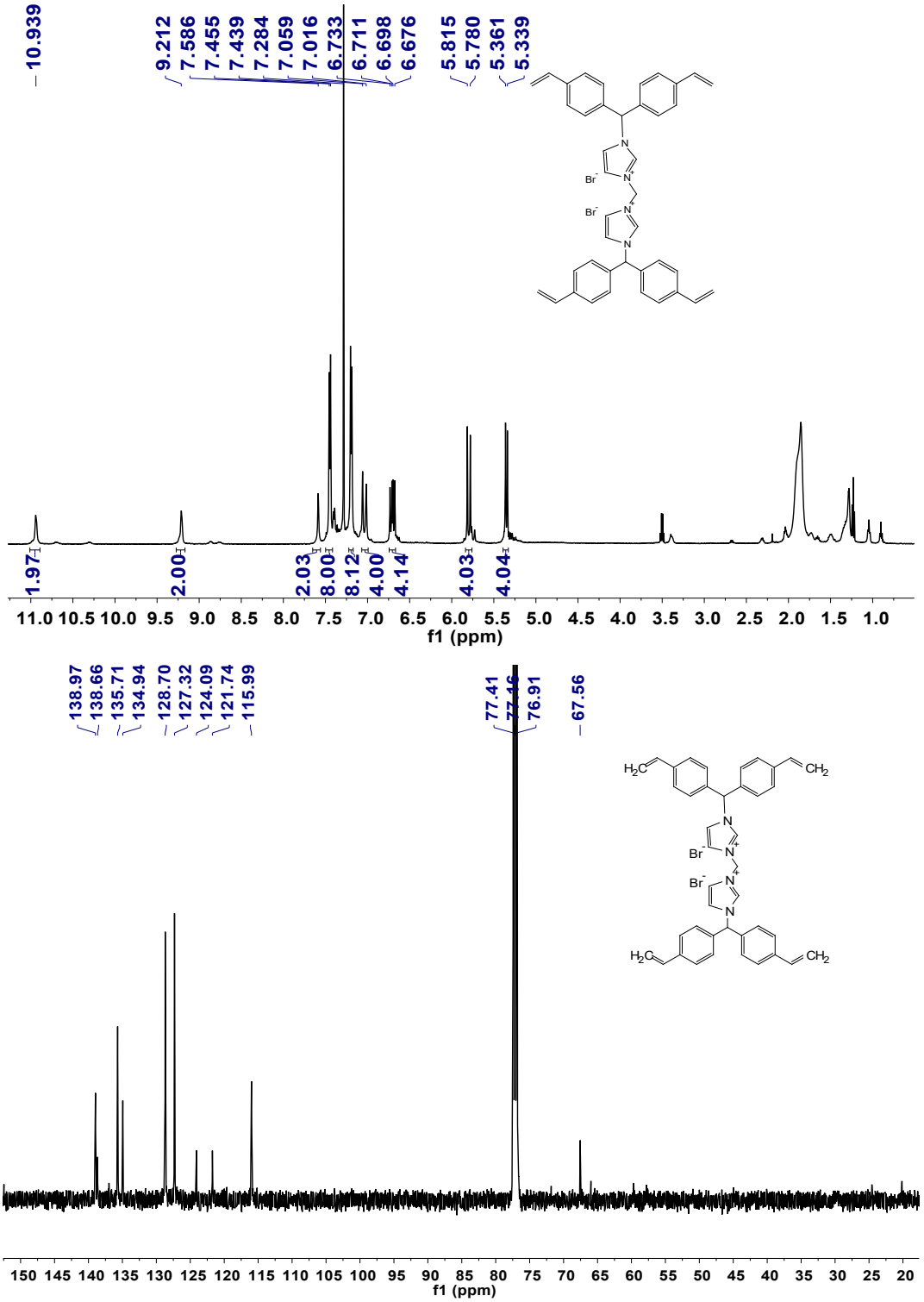

Figure S34. ^{1}H NMR spectra and ^{13}C NMR of compound **2**.

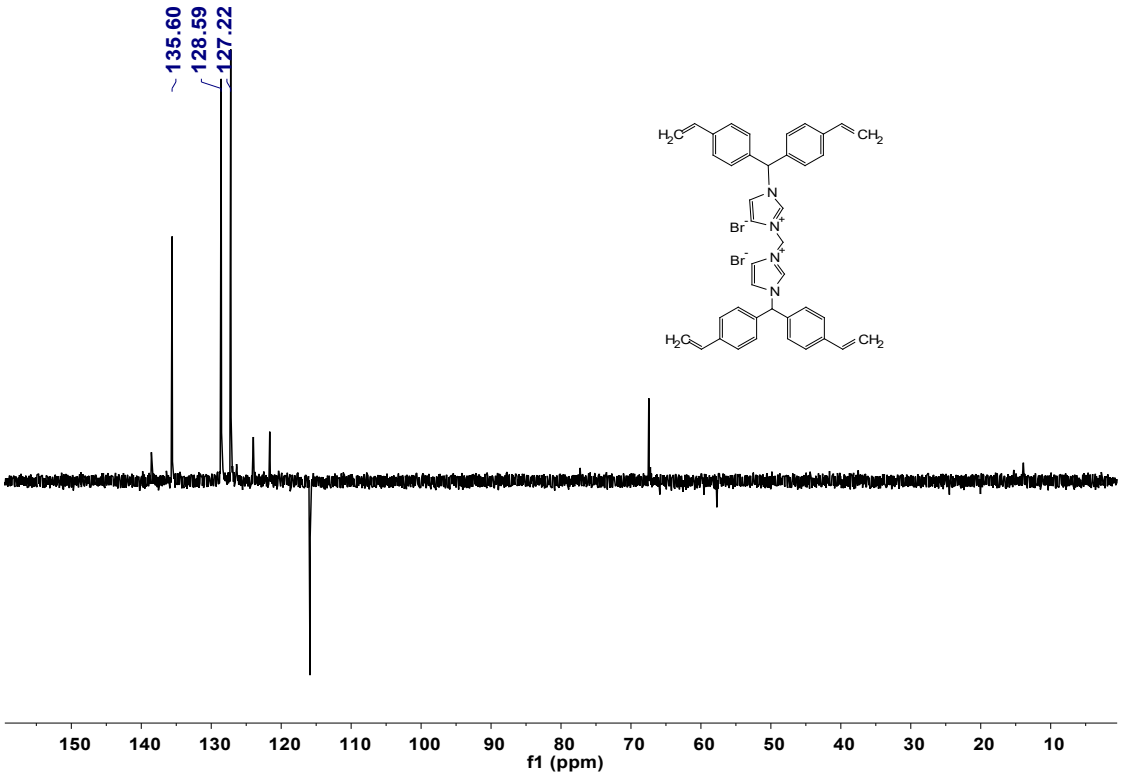

Figure S35. Distortionless enhancement by polarization transfer (DEPT) spectra of compound **2**.

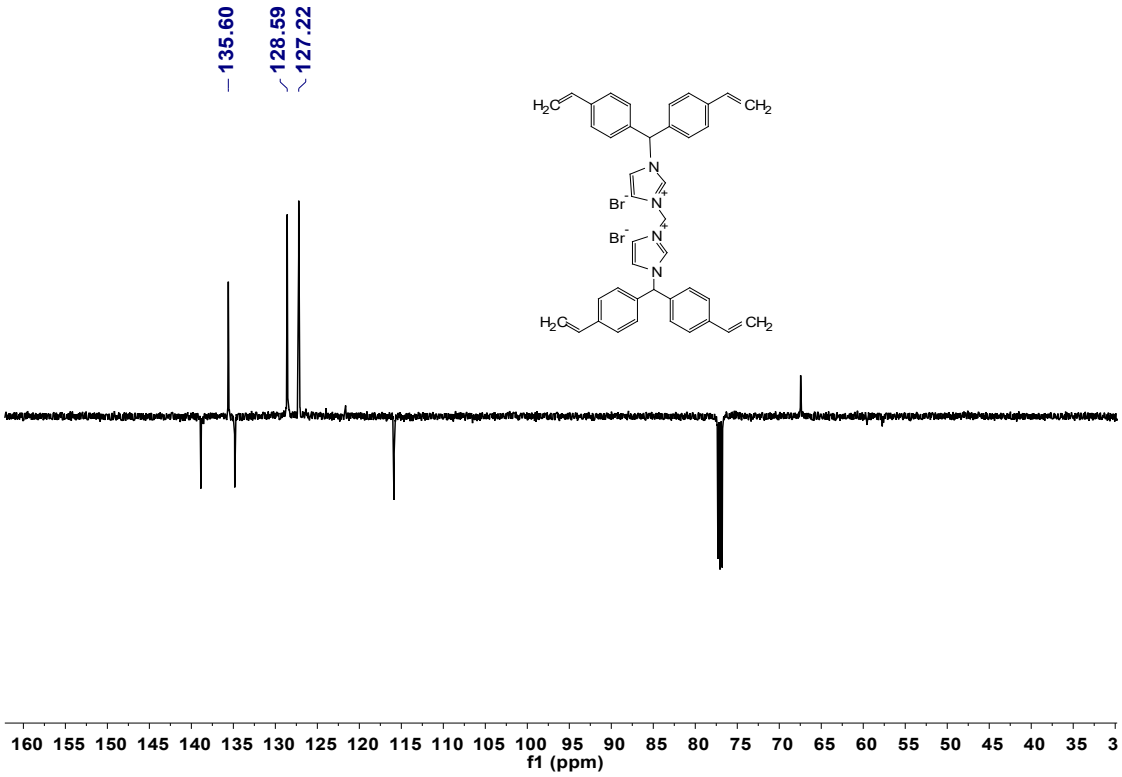

Figure S36. Attached proton test (APT) spectra of compound **2**.

5-Hydroxymethylfurfural (HMF):

^{1}H NMR (500 MHz, Chloroform-*d*) δ: 9.61 (s, 1H), 7.24 (s, 1H), 6.55 (s, 1H), 4.74 (s, 2H), 2.36 (s, 1H). ^{13}C NMR (126 MHz, Chloroform-*d*) δ: 177.70, 160.55, 152.43, 122.74, 110.03, 57.68.

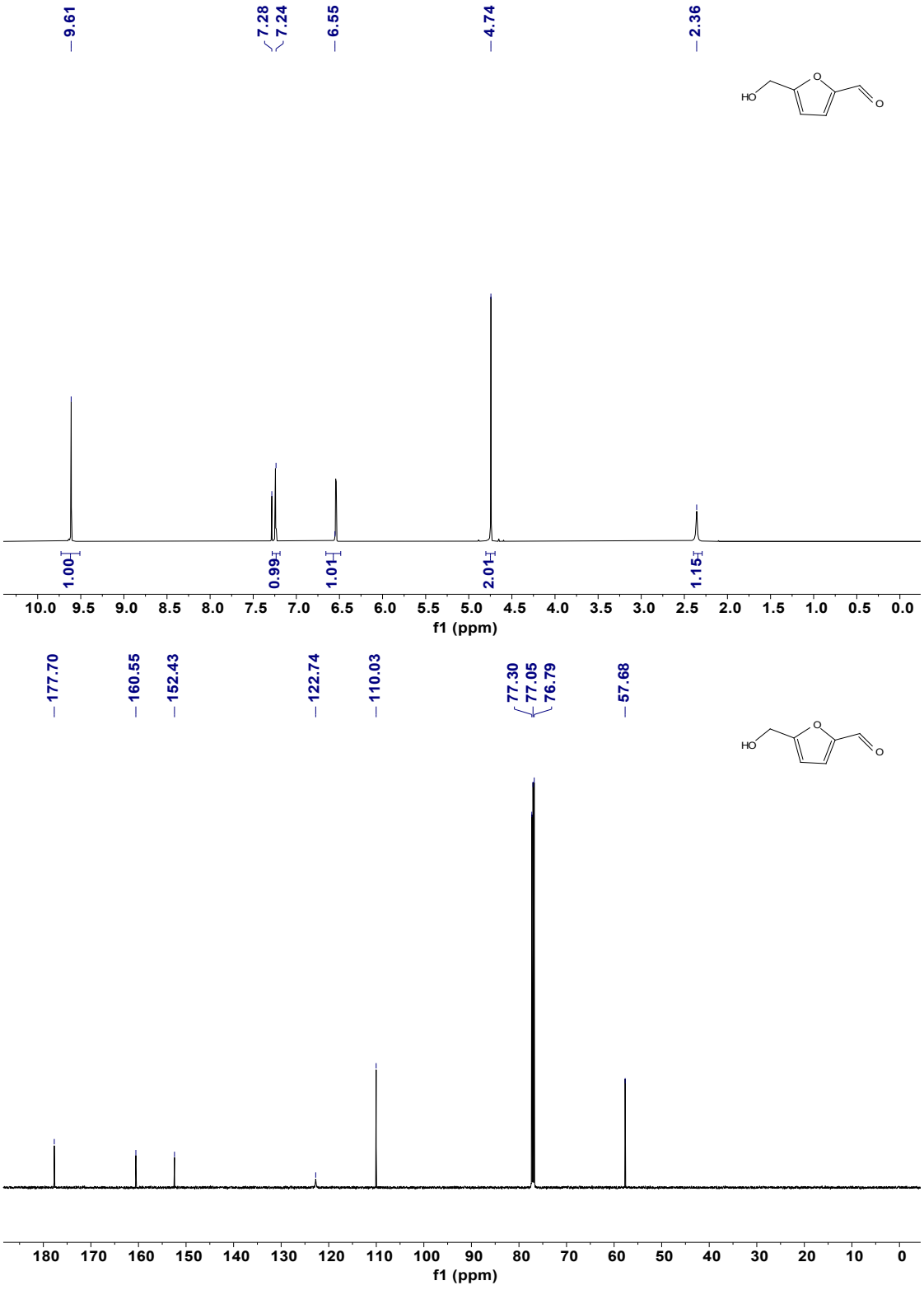

Figure S37. ^{1}H NMR and ^{13}C NMR spectra of HMF.

Furan-2,5-dicarbaldehyde (DFF):

^{1}H NMR (500 MHz, Chloroform-*d*) δ: 9.87 (s, 2H), 7.34 (s, 2H). ^{13}C NMR (126 MHz, Chloroform-*d*) δ: 179.80, 154.26, 119.16.

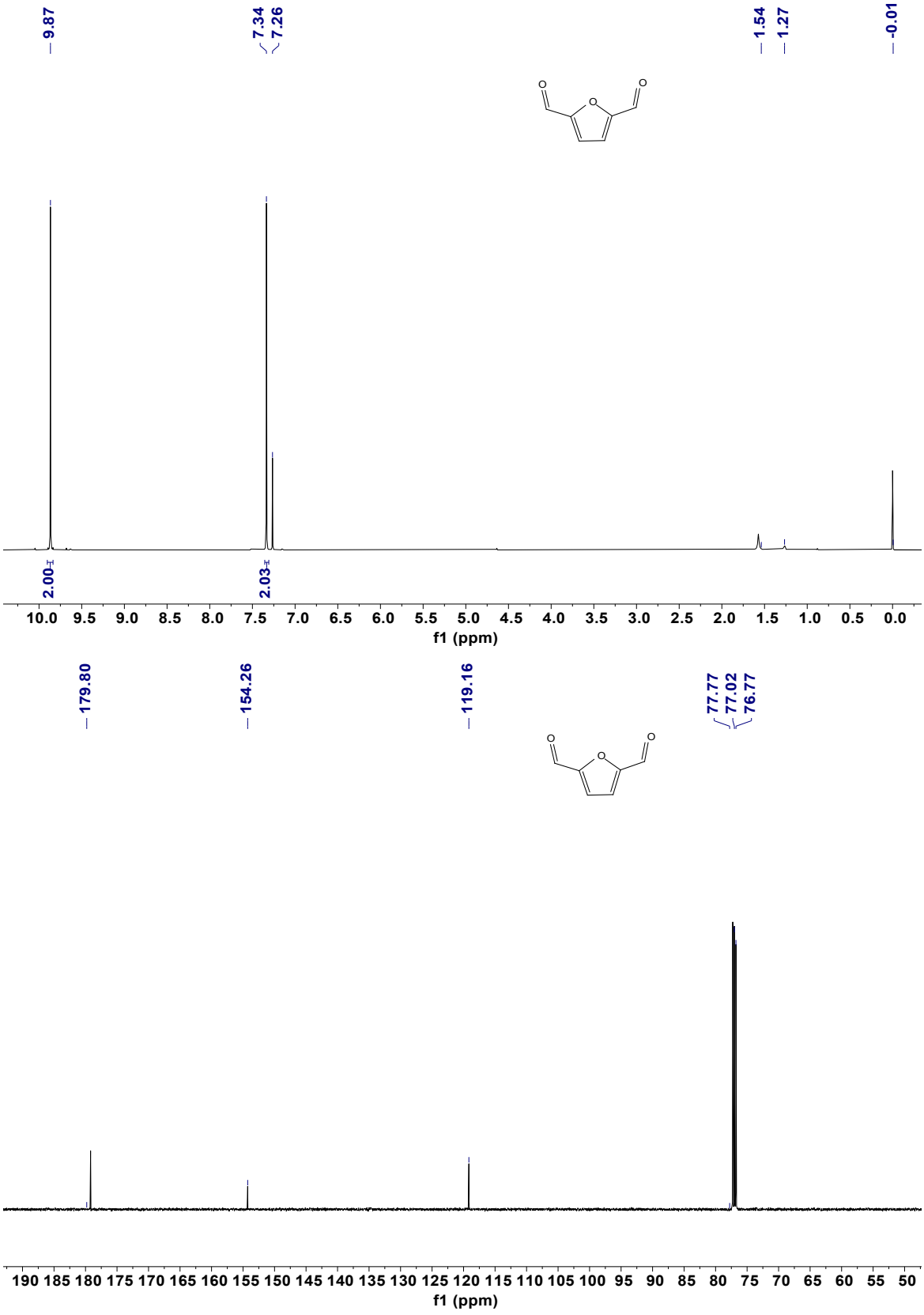

Figure S38. ^{1}H NMR and ^{13}C NMR spectra of DFF.

References

1. J. Hutter, M. Iannuzzi, F. Schiffmann, J. VandeVondole, J. cp2k: atomistic simulations of condensed matter systems. *J. Wiley Interdisciplinary Reviews-Computational Molecular Science,* 2014, **4**, 15-25.
2. G. Lippert, J. Hutter, M. Parrinello, A hybrid Gaussian and plane wave density functional scheme. *Mol. Phys.,* 1997, **92**, 477-487.
3. J. VandeVondole, M. Krack, F. Mohamed, M. Parrinello, T. Chassaing, J. Hutter, J. Quickstep: Fast and accurate density functional calculations using a mixed Gaussian and plane waves approach. *Comput. Phys. Commun.,* 2005, **167**, 103-128.
4. J. VandeVondole, J. Hutter, Gaussian basis sets for accurate calculations on molecular systems in gas and condensed phases. *Chem. Phys.,* 2007, **127**, 114105.
5. S. Goedecker, M. Teter, J. Hutter, Separable dual-space Gaussian pseudopotentials. *Phys. Rev. B.,* 1996, **54**, 1703-1710.
6. J. Perdew, K. Burke, M. Ernzerhof, Generalized Gradient Approximation Made Simple. *Phys. Rev. Lett.,* 1996, **77**, 3865-3868.
7. P. Hapala, G. Kichin, C. Wagner, F. Tautz, R. Temirov, P. Jelínek, Mechanism of high-resolution STM/AFM imaging with functionalized tips. *Phys. Rev. B,* 2014, **90**, 085421.
8. Q. Sun, S. Wang, B. Aguila, X.-J. Meng, S.-Q. Ma, F.-S. Xiao, Creating solvation environments in heterogeneous catalysts for efficient biomass conversion. *Nat. Commun.,* 2018, **9**, 3236.
9. D. Nakatake, Y. Yokote, Y. Matsushima, R. Yazaki, T. Ohshima, A highly stable but highly reactive zinc catalyst for transesterification supported by a bis(imidazole) ligand. *Green Chem.,* 2016, **18**, 1524-1530.